Graphical Abstract

Click here to download Graphical Abstract: HelmstetterGraphicalAbstract.pdf

Individual T helper cells have a quantitative cytokine memory

Caroline Helmstetter,[1,2,*] Michael Flossdorf,[3,4,*] Michael Peine,[1,2,*] Andreas Kupz,[5,6] Jinfang Zhu,[7] Ahmed N. Hegazy,[1,2,8] Maria A. Duque-Correa,[5] Qin Zhang,[3,4] Yevhen Vainshtein,[3,4] Andreas Radbruch,[2] Stefan H. Kaufmann,[5] William E. Paul,[7] Thomas Höfer,[3,4,#] and Max Löhning[1,2,#]

[1]Experimental Immunology, Department of Rheumatology and Clinical Immunology, Charité–University Medicine Berlin, 10117 Berlin, Germany

[2]German Rheumatism Research Center (DRFZ), a Leibniz Institute, 10117 Berlin, Germany

[3]Division of Theoretical Systems Biology, German Cancer Research Center (DKFZ), 69120 Heidelberg, Germany

[4]Bioquant Center, University of Heidelberg, 69120 Heidelberg, Germany

[5]Department of Immunology, Max Planck Institute for Infection Biology, 10117 Berlin, Germany

[6]Queensland Tropical Health Alliance Research Laboratory, James Cook University, Cairns Campus, Smithfield QLD 4878, Australia

[7]Laboratory of Immunology, National Institute of Allergy and Infectious Diseases, National Institutes of Health, Bethesda, MD 20892, USA

[8]Department of Gastroenterology, Hepatology and Endocrinology, Charité, 10117 Berlin, Germany

* C.H., M.F., and M.P. contributed equally to this work.

[#] T.H. and M.L. contributed equally to this work.

Running title: Quantitative cytokine memory of individual T cells

Contact: loehning@drfz.de or t.hoefer@dkfz-heidelberg.de

Summary

The probabilistic expression of cytokine genes in differentiated T helper (Th) cell populations remains ill-defined. By single-cell analyses and mathematical modeling we show that one stimulation featured stable cytokine nonproducers as well as stable producers with wide cell-to-cell variability in the magnitude of expression. Focussing on interferon-γ (IFN-γ) expression by Th1 cells, mathematical modeling predicted that this behavior reflected different cell-intrinsic capacities and not mere gene-expression noise. *In vivo*, Th1 cells sort-purified by secreted IFN-γ amounts preserved a quantitative memory for both probability and magnitude of IFN-γ reexpression for at least one month. Mechanistically, this memory resulted from quantitatively distinct transcription of individual alleles and was controlled by stable expression differences of the Th1 cell lineage-specifying transcription factor T-bet. Functionally, Th1 cells with graded IFN-γ production competence differentially activated infected macrophages for bacterial killing. Thus, individual Th cells commit to produce distinct amounts of a given cytokine, thereby generating functional intrapopulation heterogeneity.

Introduction

Cytokines are key regulators of immune responses. Differentiated T helper (Th) cells rapidly secrete specific cytokines upon antigen challenge (Lohning et al., 2002; Zhu et al., 2010). The lineage-specifying transcription factors T-bet, GATA-3, and RORγt program the expression of Th1 [(interferon (IFN)-γ], Th2 [interleukin (IL)-4, IL-5, and IL-13], and Th17 (IL-17) cell-associated cytokines, respectively (Zhu et al., 2010). However, only a fraction of activated Th cells expressing such a 'master regulator' transcription factor produces the associated cytokines (Bucy et al., 1994; Openshaw et al., 1995; Peine et al., 2013). Such intrapopulation heterogeneity has been attributed to a stochastic 'choice' of the cells (Apostolou and Thanos, 2008; Guo et al., 2005; Rand et al., 2012). However, mammalian gene transcription occurs in brief bursts, separated by random intervals of up to several hours (Harper et al., 2011; Suter et al., 2011). Thus, antigen-stimulated T cells might rapidly switch between cytokine-producing and silent states, implying that all cells in a population are producers - but at different time points. Alternatively, the decision to express a cytokine could be made only once, resulting in stable producing and nonproducing subpopulations.

A rapid-switching model based on transcriptional bursting implies that the amounts of a given cytokine produced by an individual cell fluctuate over time. Such rapid fluctuations have been observed for constitutively expressed genes in human cell lines (Sigal et al., 2006), suggesting that each individual cell recapitulates the entire variability in the population. By contrast, individual Th cells might have different inherent capacities to express cytokine genes. This capacity may be influenced by response thresholds caused by heterogeneous expression of receptors, signaling proteins, and key transcription

factors (Feinerman et al., 2008; Peine et al., 2013). Intrapopulation heterogeneity may result in functional diversification of Th cell responses (O'Garra et al., 2011) and - presumably - of T cell-mediated immunological memory.

Previous studies on cytokine expression are based on conventional 'snapshot' flow cytometry that would have missed a rapid switching between cytokine-producing and -nonproducing states. Here, we have developed an experimental method to track the expression of endogenous cytokine genes in individual Th cells over time without resorting to genetic alterations. Our approach combined the fluorescent labeling of viable cytokine producers by a cytokine capture matrix on the cell surface ('secretion assay') (Assenmacher et al., 1998; Lohning et al., 2003) with time-delayed intracellular staining. We show that in a given stimulation, T cells made a stable decision whether to produce a given cytokine or not. In addition, the producers committed to individual magnitudes of expression. Mathematical modeling predicted different cell-intrinsic capacities to express the respective cytokine genes. Using a prototypical example, we found that the amount of IFN-γ production was a stable feature of individual Th1 cells that was memorized for at least one month *in vivo*, even upon immunological challenge. This memory was based on quantitatively distinct transcription at single alleles, controlled by different quantities of T-bet protein, and associated with graded DNA methylation at the *Ifng* and *Tbx21* loci. In functional terms, the produced IFN-γ amount defined a cell's capacity to stimulate macrophages to kill bacteria. Thus, individual T cells can stably maintain and inherit distinct expression rates of a given cytokine, thereby regulating their potential to stimulate immune responses.

Results

Differentiated Th cells segregate into stable cytokine-producing and -nonproducing subsets during one stimulation

We analyzed the cytokine production behavior of Th1, Th2, and Th17 cells in a kinetic fashion. To obtain homogeneous populations, we derived them from naive precursors. Cytokine-producing cells reached their maximal frequency within ~3 h after stimulation (Fig. S1A). An interruption of stimulation led to the rapid termination of cytokine production, and resumption of stimulation caused rapid reinitiation (Fig. S1B). At all time points, a fraction of the cells did not produce cytokines. However, this behavior did not reflect heterogeneous differentiation or activation, since all cells underwent multiple cell divisions (data not shown), upregulated the activation marker CD44 (Fig. S1C), and homogeneously expressed the lineage-specifying transcription factors T-bet, GATA-3, or RORγt, respectively. Thus, cytokine expression by Th cell populations appeared heterogeneous and required recent and continuous stimulation, consistent with previous studies on $CD8^+$ T cells (Corbin and Harty, 2005; Slifka et al., 1999).

To distinguish whether all stimulated Th cells transiently produce cytokines but rapidly cycle between producing and nonproducing states or whether there are stable producing subpopulations (Fig. 1A), we tracked the behavior of individual cells over time. We surface-labeled viable cytokine producers using the cytokine secretion assay technology (Assenmacher et al., 1998; Lohning et al., 2003) and counterstained for the same cytokine intracellularly at various time points (Fig. 1B). The vast majority of Th1 cells that initiated IFN-γ production maintained it for several hours in the presence of the stimulus (Fig. 1C; top row, upper right quadrants). Controls without cell permeabilization

confirmed the accurate detection of intracellular versus surface-captured IFN-γ (Fig. S2A). Similarly, individual Th17 cells continuously produced IL-17 (Fig. S2B). A small fraction of cells switched on cytokine production with some delay (Fig. 1C, upper left quadrants), consistent with the gradual culmination of cytokine production (cf. Fig. S1A, B). Virtually all cytokine-producing cells switched off cytokine production within 21 h (Fig. 1C, lower right quadrants). A substantial fraction of cells did not produce cytokine throughout the experiment (Fig. 1C, lower left quadrants). These results show that upon stimulation, fully differentiated Th cells segregate into stable cytokine-producing and -nonproducing subpopulations.

Individual Th cells maintain their specific rate of cytokine production

To assess how long an individual cell produced a given cytokine, we fitted mathematical models of cytokine production to the data in Fig. 1C. The models describe IFN-γ^- cells becoming IFN-γ^+ upon stimulation and expressing the cytokine for a certain time. In the first model, we allowed for rapid switching between on and off states, e.g. by transcriptional bursting (Fig. 1D). We fitted the model to the fraction of IFN-γ^+ cells over time, either gating on all cells or only those that had initially been surface-labeled (Fig. 1C, 0 h, upper right gate). This fit constrained the backward rate from the transcriptionally active state, ω, to be less than 0.09/h (upper bound of the 95% confidence interval, Table S1), implying a half-life of this state of 7.7 h or longer. Hence, repeated on-off switching of IFN-γ expression could be neglected. Instead, we considered a stable-production model where switching off cytokine expression is irreversible after a Gamma-distributed production period τ (Fig. 1E). The model accurately fitted the time

courses of intracellular IFN-γ^+ cells among both total and surface-labeled cells simultaneously (Fig. 1F, G). The best-fit parameters implied that, on average, after an initial delay of 40 min, the cells start IFN-γ expression within the following 1 h and continue production for 5.9 ± 3.6 h (Fig. 1H, Table S1). Thus, to describe the data, the stable-production model was required where individual cells switch on continuous cytokine production once (cf. Fig. 1A, E). Switching on was more synchronous than switching off, explaining that the decline of the IFN-γ^+ fraction was slower than the initial increase (Fig. 1F). Stable production rather than rapid switching was also observed for IL-17 expression by Th17 cells (Fig. S 2B) and thus appeared to be a common mode of effector cytokine expression.

Mathematical modeling predicts inherently distinct cytokine expression capacities of individual cells

Among IFN-γ^+ cells, the IFN-γ amount per cell varied by more than one order of magnitude. Since our detection method introduced only a marginal experimental error (relative error 17%, Fig. 2A), this was primarily due to true cell-to-cell variability which could result from stochastic fluctuations in IFN-γ expression (e.g. in transcription rate) or intrinsically different IFN-γ expression capacities of individual cells, or both. Addressing this question, we asked if a standard stochastic gene-expression model based on transcriptional bursting could describe the data (Raj et al., 2006). To account for the transient nature of cytokine production, we extended the standard model by including initial and terminal off states (Fig. 2B). This promoter state transition model produces cell-to-cell heterogeneity in IFN-γ expression due to switching between inactive and

active promoter states [with rates rates $k_{\pm}$; (Friedman et al., 2006; Mariani et al., 2010; Miller-Jensen et al., 2011)] as well as asynchronous induction and terminal switching off of cytokine transcription (with rates k_{on} and k_{off}, respectively).

Given the short half-life of IFN-γ protein in the cells (~1 h, Fig. 2C; blue crosses), transcription fluctuations would manifest themselves at the protein level. However, the correlation of IFN-γ protein amounts at two different time points in the same cell (autocorrelation) persisted for longer than the IFN-γ protein half-life (Fig. 2D). We asked if the model in Fig. 2B could explain this autocorrelation and the observed cell-to-cell variability in IFN-γ expression, as quantified by the coefficients of variation of the IFN-γ^+ cells (Fig. 2E, blue crosses). Systematic parameter estimation (Table S1) revealed that the model accounted for the kinetics of IFN-γ^+ cells (Fig. 2C, red curves) as well as the temporal correlations of IFN-γ quantities in individual cells (Fig. 2D, red curve) but failed to reproduce the cell-to-cell variability of IFN-γ expression. The model accounted neither for the width (Fig. 2E) nor the shape of the distribution (Fig. 2F). Thus, intrinsic noise in gene expression alone could not explain the observed cell-to-cell variability of IFN-γ expression.

Therefore, we extended the model by cell-to-cell differences in the IFN-γ expression capacity, defined as the product of transcription and translation rate (Fig. 2G, H). These differences would result from the variability in regulators of transcription and/or translation between the cells, including epigenetic mechanisms. Moreover, as we found that transcriptional bursting (rates $k_{\pm}$) made a negligible contribution to the protein variability, explaining <7% of the CV of the IFN-γ^+ cells (Table S1), we neglected it. The resulting distributed production capacity model accurately described the dynamics of

IFN-γ expression upon stimulation (Fig. 2I). In the beginning, the broad IFN-γ distribution was due to the distributed expression capacities while the further increase until t = 3 h resulted from the different switching-off times of individual cells. We also fitted the model to the distribution of initially surface-labeled cells, achieving a good fit with the same parameter values (Fig. S3). To conclude, the observed cell-to-cell variability in IFN-γ protein amounts is consistent with a model in which individual cells have inherently distinct capacities for IFN-γ expression.

Individual Th1 cells exhibit a stable quantitative memory for IFN-γ and T-bet expression

According to our data-driven modeling, a given antigen stimulation of Th1 cells featured stable IFN-γ high producers, low producers, and nonproducers. We thus hypothesized that the stability of these qualitative (decision to express) and quantitative (expression magnitude) characteristics might persist in subsequent stimulations. To generate IFN-γ–producing cells *in vivo*, we adoptively transferred naive lymphocytic choriomeningitis virus (LCMV)-T cell receptor (TCR)-transgenic (tg) Th cells into wild-type (WT) mice and infected the recipients with LCMV, a strongly Th1-polarizing pathogen (Hegazy et al., 2010). At the peak of infection, we isolated the transferred cells, which all expressed T-bet (Fig. 3A, histogram), and sorted them by secreted amounts of IFN-γ upon antigen-specific restimulation (Fig. 3B). In a second restimulation 4 d later, those cells that had initially produced the highest amounts of IFN-γ showed a higher probability to reexpress it than sorted IFN-γ^{lo} or IFN-γ^{-} cells, and they again produced more IFN-γ per cell (Fig. 3C). IFN-γ^{hi} cells also expressed the highest amounts of T-bet directly after sorting (data

not shown), and this correlation was stable for at least 4 d (Fig. 3D). Thus, individual Th1 cells generated during a viral infection *in vivo* had a quantitative memory for IFN-γ production that correlated with their degree of T-bet expression. Moreover, kinetic analyses revealed that the graded IFN-γ production capacity of IFN-γ–sorted Th1 cells was a stable property that could be observed at every time point in daily restimulations (Fig. 3E, F, Fig. S4).

Even among Th1 cells that were strongly polarized in LCMV infections, some did not produce IFN-γ in every restimulation (cf. Fig. 3B). To formally show that fully differentiated Th1 cells had a quantitative cytokine memory, we performed a similar sort-and-track experiment starting with purified IFN-γ producers. Again, individual cells memorized both probability and per-cell amount of IFN-γ production, and this correlated with their degree of T-bet expression (Fig. S5). Thus, the probability and amount of IFN-γ expression are stable properties of *bona fide* Th1 cells.

The quantitative memory for IFN-γ expression persists upon viral challenge infection *in vivo*

To analyze if quantitative differences in IFN-γ expression were long-term stable in memory Th1 cells *in vivo*, we adoptively transferred purified IFN-γ^{hi}, IFN-γ^{lo}, or IFN-γ^{-} Th1 cells into WT mice. After more than one month, we analyzed the capacity of the resting cells to reexpress IFN-γ. Both probability and per-cell expression still recapitulated the IFN-γ expression capacity which the cells had been sorted by (Fig. 3G). In addition, T-bet expression was still positively correlated with the amount of IFN-γ production (Fig. 3H). Thus, the magnitude of expression of both T-bet (a constitutively

expressed transcription factor) and IFN-γ (a stimulation-induced cytokine) are stable cell-intrinsic features.

We then examined if individual Th1 cells maintain their quantitative cytokine memory after a strongly Th1-polarizing challenge. We isolated *in vivo*-differentiated Th1 cells from LCMV-infected mice, sorted them by secreted quantities of IFN-γ, and transferred the sorted fractions into naive recipients (Fig. 3I). After at least two weeks of resting, the recipient mice were infected with LCMV. Upon reisolation at the peak of the secondary infection, the cells still recapitulated their initial graded differences in IFN-γ expression probability and amount (Fig. 3J). Notably, the stably constrained IFN-γ production of the sorted IFN-γ^- cells was not due to impaired proliferation, since these cells expanded at least 50-fold upon LCMV challenge. Thus, differentiated Th cells can remain committed to produce distinct quantities of effector cytokines while participating in sequential immune reactions *in vivo*.

The quantitative memory for IFN-γ production is regulated at the level of transcription at individual alleles

Next, we asked whether the quantitative cytokine memory was regulated at the RNA or protein level. Th1 cells sorted by their amount of IFN-γ secretion continuously featured graded IFN-γ mRNA quantities in subsequent restimulations (Fig. 4A), matching their stably graded IFN-γ protein amounts and probabilities to produce IFN-γ (cf. Fig. 3E, F, Fig. S4). Thus, the secretion of distinct amounts of IFN-γ by subpopulations of Th1 cells does not reflect different translation rates but different mRNA amounts. To distinguish the possibility of enhanced transcription at the *Ifng* locus in IFN-γ^{hi} cells from that of

enhanced IFN-γ mRNA degradation in IFN-γ^{lo} cells, we used the transcription inhibitor actinomycin D. Blocking transcription 3 h after stimulation onset reduced IFN-γ mRNA (Fig. 4B). However, this reduction was most profound in IFN-γ^{hi} cells, showing that degradation was at least as efficient in IFN-γ^{hi} cells as in IFN-γ^{lo} cells. Moreover, already 15 minutes after stimulation onset, when mRNA amounts reflect transcription rather than degradation rates, IFN-γ transcripts were graded among the sorted subsets (Fig. 4C). Taken together, these results indicate that the specific amounts of IFN-γ secreted by individual Th1 cells resulted from differences in IFN-γ transcription rates and not from differences in mRNA degradation or translation.

One possible mechanism underlying *Ifng* gene expression differences could be stable usage of either one or two alleles, such that IFN-γ^{hi} cells would always express biallelically while IFN-γ^{lo} cells would only express monoallelically. To test this hypothesis, we differentiated *Ifng*$^{+/+}$ and *Ifng*$^{+/-}$ Th1 cells in a co-culture and sorted them for differential IFN-γ secretion. We found that the graded differences in IFN-γ expression were similarly stable in WT and *Ifng*$^{+/-}$ cells (Fig. 4D). Thus, it is not differential allelic usage but constant transcription rate differences at individual alleles that regulate the quantitative memory for IFN-γ. These cell-specific transcription rates could result from different chromatin states allowing distinct degrees of transcription factor binding at regulatory sites. One mechanism assumed to stably suppress transcription is DNA methylation. We found less methylation in IFN-γ^{hi} and IFN-γ^{lo} cells than in IFN-γ^{-} Th1 cells at the key regulatory conserved noncoding sequence (CNS) -6 (Balasubramani et al., 2010b; Shnyreva et al., 2004) at the *Ifng* locus (Fig. 4E). We also found graded DNA methylation upstream of the *Tbx21* promoter (Fig. 4E), matching the higher T-bet

expression in IFN-γ^{hi} cells compared with that in their IFN-$\gamma^{lo/-}$ counterparts (cf. Fig. 3D, F). In summary, our findings imply a model where DNA methylation differences contribute to quantitatively distinct IFN-γ transcription rates at individual alleles.

T-bet quantitatively controls IFN-γ expression in fully differentiated Th1 cells

Cells sorted for a high amount of IFN-γ secretion had more T-bet mRNA and protein than their IFN-γ^{lo} and IFN-γ^{-} counterparts (Fig. S6, Fig. 3D, H). This corresponds with the more pronounced DNA methylation of IFN-γ^{lo} and IFN-γ^{-} cells at the *Tbx21* locus (cf. Fig. 4E). Next, we analyzed the quantitative relationship between T-bet and IFN-γ expression in fully committed Th1 cells at the single-cell level by coexpression analysis. We found that the more T-bet protein was expressed by a cell, the higher were its probability to produce IFN-γ and the produced IFN-γ amount (Fig. 5A). To test if T-bet amounts are predictive of IFN-γ expression in subsequent restimulations, we sorted Th1 cells from T-bet–ZsGreen reporter (TBGR) mice (Zhu et al., 2012) by their intensity of ZsGreen (i.e. T-bet) expression (Fig. 5B) and analyzed their capacity to express IFN-γ. The initial T-bet expression predicted the production of IFN-γ in terms of probability and amount per cell right after the sort and also several days later (Fig. 5C, D). Upon adoptive transfer into WT mice, Th1 cells sorted by T-bet amounts preserved their differential T-bet and IFN-γ expression for at least a month *in vivo* (Fig. 5E, F). Distinct T-bet protein amounts were stably maintained by these resting memory cells independent of restimulation (Fig. S6C). Moreover, the same functional relationship between T-bet and IFN-γ expression described the data both directly after the sort and 4 weeks later (Fig.

5G), suggesting that T-bet quantitatively controlled IFN-γ expression in the same manner in activated effector and in memory cells.

T-bet had been identified as the master regulator of the Th1 cell lineage because of its capacity to instruct non-Th1 cells to acquire IFN-γ production competence (Szabo et al., 2000). To address if a causal relationship dictated the quantitative correlation between T-bet protein and IFN-γ production in fully committed, already IFN-γ–competent Th1 cells, we sorted Th1 cells for different amounts of IFN-γ secretion (and thus indirectly also for different T-bet expression). We then further increased their respective T-bet amount by retroviral overexpression (Fig. 6A). Notably, all of these Th1 cells stained positive for T-bet protein already before the transduction (cf. Fig. S1C and hCD4^{-} cells in Fig. 6D). Upon T-bet overexpression, sorted IFN-γ^{hi}, IFN-γ^{lo}, and IFN-γ^{-} Th1 cells exhibited a strong increase in both probability and per-cell amount of IFN-γ production compared with their counterparts that were transduced with a control retrovirus (Fig. 6B, C). Both quantitative parameters were also graded among unsorted T-bet–overexpressing cells, correlating with the degree of ectopic T-bet expression (Fig. 6D, E). Taken together, an increase in T-bet amount in already T-bet^{+} Th1 cells can overcome an otherwise stably restrained cellular capacity to produce IFN-γ. This result identifies T-bet as a quantitative regulator of IFN-γ expression in fully differentiated Th1 cells.

Graded IFN-γ production by Th1 cells regulates bacteria killing by macrophages

To test the functional capacity of Th1 cells with distinct IFN-γ production, we analyzed their ability to activate macrophages for bacteria killing. We infected macrophages with the facultative intracellular pathogen *Salmonella enterica* serovar Typhimurium (*S.*

Typhimurium) and co-cultured them with sorted IFN-γ^{hi}, IFN-γ^{lo}, or IFN-γ^{-} Th1 cells (Fig. 7A). IFN-γ^{hi} Th1 cells were most efficient in inducing bacterial killing, followed by IFN-γ^{lo} and finally IFN-γ^{-} Th1 cells (Fig. 7B). Graded bacterial killing was associated with different nitric oxide (NO) production by the macrophages (Fig. 7C). *Ifngr1*$^{-/-}$ macrophages could not kill the bacteria nor produce NO when co-cultured with either Th1 cell population (Fig. 7B, C, right graphs), demonstrating that the effects were IFN-γ–dependent. The IFN-γ amount secreted by IFN-γ^{hi} and IFN-γ^{lo} Th1 cells differed by two orders of magnitude (Fig. 7D). Thus, in addition to the frequency of cytokine producers in a population, the per-cell amount of cytokine production critically influences the functional capacity of Th cells to control intracellular bacterial infections.

Discussion

While cytokines have been recognized for more than three decades as key effector molecules of T cells, quantitative aspects of their expression and underlying regulatory mechanisms are poorly understood. Here, we have shown that the well-known phenomenon of a heterogeneous cytokine production within a cell population is caused by stable cellular decisions and not governed by short-term transcription noise (Suter et al., 2011). We found that during an antigenic challenge, individual Th cells expressed their effector cytokines in stable amounts that vary widely between cells. Focusing on IFN-γ as a prototypical cytokine, we demonstrated that the magnitude of its expression per-cell was an intrinsic feature of Th1 cells. *In vivo*, this magnitude was maintained by the cells and their progeny for weeks, even in the face of a strongly Th1-polarizing challenge infection that was expected to reduce cell-to-cell differences. Moreover, the expression magnitude of the Th1 cell-specific, *Ifng*-transactivating transcription factor T-bet, was also a stable and heritable quantitative feature of individual Th1 cells. It predicted the magnitude of IFN-γ expression according to a dose-response function. Thus, T cells can quantitatively control a key effector function in a stable manner by quantitatively regulating a 'master regulator' transcription factor.

How is such intrapopulation heterogeneity established? A TCR repertoire with diverse antigen affinities is likely to contribute (Constant and Bottomly, 1997) but is not required, given that we found similar heterogeneity within TCR-transgenic T cell populations. As Th1 cell differentiation proceeds, co-operative actions of STAT4 as well as T-bet together with the transcription factors Hlx and Runx3 induce permissive chromatin remodeling at the *Ifng* locus (Balasubramani et al., 2010a). The cell-specific

fine-tuning of this process may be achieved by the regulation of cytokine signaling. This can occur through the control of either the expression of cytokine receptors or the availability and/or activity of downstream signal transduction molecules and transcription factors. Indeed, quantitative regulation of IL-12Rβ2 and STAT4 (Szabo et al., 1997; Usui et al., 2003) as well as of IFN-γR expression (de Weerd and Nguyen, 2012) during Th cell differentiation have been described, e.g. due to asymmetric cell division (Chang et al., 2007). Such kinds of adjustment may generate Th1 effector cells with distinct IFN-γ production probabilities at the population level and distinct IFN-γ as well as T-bet expression rates in individual cells. We found that the probability to express IFN-γ and its amount produced per cell were heterogeneous in Th1 cell populations, and both features were stably memorized by individual cells. We did not detect a correlation between the IFN-γ expression of sorted cell populations and their survival *in vivo*. In extension of our previous study (Lohning et al., 2008), this finding indicated that IFN-γ^{hi} cells did not represent short-lived effectors but could efficiently form a memory compartment.

Upon lineage commitment, the loci of signature cytokines exhibit stable lineage-specific epigenetic marks (Wei et al., 2009), allowing the rapid reexpression of the appropriate effector cytokines. However, key transcription factors continuously serve important regulatory functions. In fully differentiated Th2 cells, GATA-3 remains crucial for IL-13 and IL-5 production, although it appears largely dispensable for IL-4 production (Zhu et al., 2004). Overexpression of a dominant-negative T-bet mutant is most detrimental during early Th1 cell differentiation, but still results in a significant decrease of IFN-γ production per cell when introduced after sequential polarizations with IL-12 (Martins et al., 2005). We found that, although all Th1 cells expressed T-bet, its protein amounts

varied in the effector population, and these differences were stably maintained in memory cells *in vivo*. Consistent with a continuous requirement of T-bet for efficient *Ifng* expression, we showed that IFN-γ production increased even in fully committed Th1 cells as a direct consequence of a retrovirus-induced gradual T-bet overexpression. Thus, T-bet does not only orchestrate the commitment of naive T cells to the Th1 cell differentiation program but continuously serves as a quantitative regulator of Th1 cell functions.

How does T-bet quantitatively control IFN-γ expression in memory Th1 cells? Recent studies indicate that epigenetic marks are subjected to a certain turnover and have to be actively maintained (Barth and Imhof, 2010; Dalton and Bellacosa, 2012). Here, T-bet seems a likely candidate as it contributes to the opening of the *Ifng* locus during primary Th1 cell differentiation (Mullen et al., 2001; Szabo et al., 2000). We found that stable IFN-γ expression differences were associated with corresponding DNA methylation patterns at both the *Ifng* and *Tbx21* loci. In addition to DNA methylation, various histone modifications are thought to orchestrate gene expression activity (Barth and Imhof, 2010). The graded DNA methylation we observed at CNS -6 of the *Ifng* gene and at the *Tbx21* promoter may partially contribute to a stable quantitative cytokine memory. However, we hypothesize that a quantitative cytokine memory is rather based on a combination of multiple permissive and repressive epigenetic modifications at several regulatory sites. They may act together with distinct T-bet expression rates retained by the cells through transcriptional autoactivation (Afkarian et al., 2002; Mullen et al., 2001). Moreover, T-bet may co-operate with NF-κB family members to facilitate *Ifng* expression upon antigen-driven restimulation – in analogy to STAT4 enabling NF-κB

binding to the IFN-γ locus (Balasubramani et al., 2010b) in the scenatio of IL-12– and IL-18–driven antigen-independent IFN-γ expression by Th1 cells (Robinson et al., 1997). Furthermore, cytokine expression may generally include a stochastic element (Zhao et al., 2012). Then, changes of the expression probability would require a regulator, and the maintenance of a cell's individual production magnitude of this regulator would constitute a quantitative cytokine memory. Here, distinct amounts of transcriptional repressors such as twist1 (Niesner et al., 2008; Pham et al., 2012) could contribute to the stable differences in IFN-γ expression between individual Th1 cells. We found a major regulatory step to generate these differences already at the level of transcription, controlled by the positive regulator T-bet. Thus, we suggest that posttranscriptional mechanisms such as different mRNA decay rates or modulation by microRNAs are unlikely to be key mechanisms.

Cytokine genes can be expressed either mono- or biallelically (Guo et al., 2005; Hu-Li et al., 2001). Therefore, graded cytokine expression rates might be the result of transcription from either one or two alleles. However, we found that even cells with only one functional *Ifng* allele maintained quantitative expression differences. This proves that not allelic usage but different transcription at individual alleles constitutes the decisive mechanism underlying a cell's quantitative cytokine memory.

While the frequency of cytokine-producing cells within a population and the expression per cell both matter for the local cytokine concentration, most studies focus exclusively on the former. Yet, we found that Th1 cells exhibiting a mere 3-5-fold difference in their IFN-γ secretion later accumulated to a 100-fold difference over time. Thus, relatively

small per-cell differences in the production magnitude of a given cytokine likely have a great impact on immune responses.

IFN-γ is crucial for the control of *Salmonella* infections (Eckmann and Kagnoff, 2001). We observed that distinct IFN-γ expression rates of Th1 cells translated into graded activation of infected macrophages to kill intracellular bacteria. Hence, the amount of IFN-γ produced by individual Th1 cells was decisive for the functional outcome of the T-cell–macrophage interaction. Thus, a population of seemingly homogeneously differentiated T cells indeed features stable functional diversity that could quantitatively regulate various immune reactions. This mechanism might also provide a possibility to limit immunopathology. Under changing environmental challenges, plasticity of Th cell programs can be beneficial (Hegazy et al., 2010). IFN-γ^{lo} Th1 cells express T-bet only modestly and thus might retain certain plasticity, e.g. to adjust to a second pathogen that shares an epitope with the first but requires a different type of immune response.

Cytokine production must be controlled tightly, since a misbalance can induce pathology. Here, we have demonstrated that individual T cells stably commit to express distinct amounts of a given cytokine. This fine-tuning of cytokine production could contribute to the regulation of immune responses and the prevention of excessive inflammation. The persistent memory for individual IFN-γ expression rates shown here could result from regulation at several levels. Yet, the specific amount of T-bet produced by a Th1 cell is decisive for its IFN-γ expression magnitude. With regard to potential clinical application, individual rates of cytokine and/or transcription factor expression could serve as predictive markers for the quantitative functional behavior of T cells and their progeny in

later antigenic challenges. These findings could lead to therapeutic strategies to improve the protective capacity of T cell responses and dampen associated immunopathology.

Experimental procedures

Mice

DO11.10 ovalbumin-TCR^{tg} mice, *Ifngr1*$^{-/-}$, LCMV-TCR^{tg} (SMARTA1) Thy1.1^{+} mice, or TBGR mice (Zhu et al., 2012) crossed to SMARTA1 Thy1.1^{+} mice were used as organ donors. C57BL/6 mice or TBGR Thy1.2^{+} mice were used as recipients for cell transfers. Mice were bred under SPF conditions at the Charité animal facility, Berlin. All mouse experiments were performed in accordance with the German law for animal protection and with permission from the local veterinary offices. For details, see Supplemental Information.

Viruses and bacteria

LCMV. Mice were infected intravenously with 200 plaque-forming units.

S. Typhimurium. Macrophages were infected with an MOI of 1:10 and co-cultured with IFN-γ–sorted Th1 cells for 36 h. Macrophage lysate was plated onto LB agar plates. Bacterial colonies were counted after 24 h. For details, see Supplemental Information.

Primary T cell cultures

Naive CD4^{+}CD62L^{hi}CD44^{lo} T cells were differentiated into Th1 cells using 3 ng/ml IL-12 and 10 µg/ml anti–IL-4 (11B11), into Th2 cells using 30 ng/ml IL-4, 10 µg/ml anti–IL-12 (C17.8), and 10 µg/ml anti–IFN-γ (AN18.17.24), or into Th17 cells using 20 ng/ml IL-6, 1 ng/ml TGF-β, 10 ng/ml IL-23, 10 µg/ml anti–IL-4, and 10 µg/ml anti–IFN-γ. Cells were analyzed on d 5. For details, see Supplemental Information.

Flow cytometry

Cells were stained as described (Hegazy et al., 2010). Antibodies and buffers were purchased from eBioscience and BD Biosciences. For detailed protocols and antibody clones, see Supplemental Information.

For cytokine production analysis, cells were restimulated with PMA and ionomycin. To normalize the per cell cytokine protein amount of sorted cell populations, the geometric mean (GM) of cytokine-positive cells in a sorted subset was divided by the GM of the respective cytokine-positive cells from an unsorted population.

For transcription factor protein quantification, GM indices were calculated as the GM of stained cells divided by the GM of isotype control-stained cells. Unless indicated otherwise, GM indices of sorted cell subsets were normalized to those of unsorted cells.

Bone marrow (BM)–derived macrophages

BM from WT or *Ifngr1*$^{-/-}$ mice was cultured using standard macrophage differentiation protocols. For details, see Supplemental Information.

Cytokine secretion assay

The cytometric cytokine secretion assay was performed as described (Assenmacher et al., 1998; Lohning et al., 2003) upon PMA and ionomycin restimulation unless indicated otherwise. For details, see Supplemental Information.

Retroviral transduction

Ecotrophic retroviruses (encoding pMSCV-Tbet-I-hCD4 or pMSCV-I-hCD4) were generated by transfection of Phoenix cells. Retrovirus supernatants were used to spin-infect T cells in the presence of 8 µg/ml polybrene (Sigma).

RNA isolation and real-time PCR

RNA isolation and qPCR were performed using standard protocols. For details, see Supplemental Information.

Cytokine analysis in culture supernatants

IFN-γ concentrations in cell culture supernatants were determined by cytometric Bead Array (BD Biosciences) according to the manufacturer's instructions.

Bisulfite sequencing

DNA was isolated using the NucleoSpin Blood Kit (Macherey-Nagel). Amplicon design and bisulfite sequencing was performed by Epiontis GmbH, Berlin, Germany.

Statistical analysis

Two groups were compared with two-tailed unpaired Student's t test; n.s., not significant; *, $P < 0.05$; **, $P < 0.01$; ***, $P < 0.001$.

Mathematical modeling

For detailed description of all mathematical models, see Supplemental Information.

References

Afkarian, M., Sedy, J.R., Yang, J., Jacobson, N.G., Cereb, N., Yang, S.Y., Murphy, T.L., and Murphy, K.M. (2002). T-bet is a STAT1-induced regulator of IL-12R expression in naive CD4+ T cells. Nat Immunol *3*, 549-557.

Apostolou, E., and Thanos, D. (2008). Virus Infection Induces NF-kappaB-dependent interchromosomal associations mediating monoallelic IFN-beta gene expression. Cell *134*, 85-96.

Assenmacher, M., Lohning, M., Scheffold, A., Manz, R.A., Schmitz, J., and Radbruch, A. (1998). Sequential production of IL-2, IFN-gamma and IL-10 by individual staphylococcal enterotoxin B-activated T helper lymphocytes. Eur J Immunol *28*, 1534-1543.

Balasubramani, A., Mukasa, R., Hatton, R.D., and Weaver, C.T. (2010a). Regulation of the Ifng locus in the context of T-lineage specification and plasticity. Immunological reviews *238*, 216-232.

Balasubramani, A., Shibata, Y., Crawford, G.E., Baldwin, A.S., Hatton, R.D., and Weaver, C.T. (2010b). Modular utilization of distal cis-regulatory elements controls Ifng gene expression in T cells activated by distinct stimuli. Immunity *33*, 35-47.

Barth, T.K., and Imhof, A. (2010). Fast signals and slow marks: the dynamics of histone modifications. Trends Biochem Sci *35*, 618-626.

Bucy, R.P., Panoskaltsis-Mortari, A., Huang, G.Q., Li, J., Karr, L., Ross, M., Russell, J.H., Murphy, K.M., and Weaver, C.T. (1994). Heterogeneity of single cell cytokine gene expression in clonal T cell populations. J Exp Med *180*, 1251-1262.

Chang, J.T., Palanivel, V.R., Kinjyo, I., Schambach, F., Intlekofer, A.M., Banerjee, A., Longworth, S.A., Vinup, K.E., Mrass, P., Oliaro, J.*, et al.* (2007). Asymmetric T lymphocyte division in the initiation of adaptive immune responses. Science *315*, 1687-1691.

Constant, S.L., and Bottomly, K. (1997). Induction of Th1 and Th2 CD4+ T cell responses: the alternative approaches. Annu Rev Immunol *15*, 297-322.

Corbin, G.A., and Harty, J.T. (2005). T cells undergo rapid ON/OFF but not ON/OFF/ON cycling of cytokine production in response to antigen. J Immunol *174*, 718-726.

Dalton, S.R., and Bellacosa, A. (2012). DNA demethylation by TDG. Epigenomics *4*, 459-467.

de Weerd, N.A., and Nguyen, T. (2012). The interferons and their receptors--distribution and regulation. Immunology and cell biology *90*, 483-491.

Eckmann, L., and Kagnoff, M.F. (2001). Cytokines in host defense against Salmonella. Microbes Infect *3*, 1191-1200.

Feinerman, O., Veiga, J., Dorfman, J.R., Germain, R.N., and Altan-Bonnet, G. (2008). Variability and robustness in T cell activation from regulated heterogeneity in protein levels. Science *321*, 1081-1084.

Friedman, N., Cai, L., and Xie, X.S. (2006). Linking stochastic dynamics to population distribution: an analytical framework of gene expression. Phys Rev Lett *97*, 168302.

Guo, L., Hu-Li, J., and Paul, W.E. (2005). Probabilistic regulation of IL-4 production. J Clin Immunol *25*, 573-581.

Harper, C.V., Finkenstadt, B., Woodcock, D.J., Friedrichsen, S., Semprini, S., Ashall, L., Spiller, D.G., Mullins, J.J., Rand, D.A., Davis, J.R., and White, M.R. (2011). Dynamic analysis of stochastic transcription cycles. PLoS Biol *9*, e1000607.

Hegazy, A.N., Peine, M., Helmstetter, C., Panse, I., Frohlich, A., Bergthaler, A., Flatz, L., Pinschewer, D.D., Radbruch, A., and Lohning, M. (2010). Interferons direct Th2 cell reprogramming to generate a stable GATA-3(+)T-bet(+) cell subset with combined Th2 and Th1 cell functions. Immunity *32*, 116-128.

Hu-Li, J., Pannetier, C., Guo, L., Lohning, M., Gu, H., Watson, C., Assenmacher, M., Radbruch, A., and Paul, W.E. (2001). Regulation of expression of IL-4 alleles: analysis using a chimeric GFP/IL-4 gene. Immunity *14*, 1-11.
Lohning, M., Hegazy, A.N., Pinschewer, D.D., Busse, D., Lang, K.S., Hofer, T., Radbruch, A., Zinkernagel, R.M., and Hengartner, H. (2008). Long-lived virus-reactive memory T cells generated from purified cytokine-secreting T helper type 1 and type 2 effectors. J Exp Med *205*, 53-61.
Lohning, M., Richter, A., and Radbruch, A. (2002). Cytokine memory of T helper lymphocytes. Adv Immunol *80*, 115-181.
Lohning, M., Richter, A., Stamm, T., Hu-Li, J., Assenmacher, M., Paul, W.E., and Radbruch, A. (2003). Establishment of memory for IL-10 expression in developing T helper 2 cells requires repetitive IL-4 costimulation and does not impair proliferation. Proc Natl Acad Sci U S A *100*, 12307-12312.
Mariani, L., Schulz, E.G., Lexberg, M.H., Helmstetter, C., Radbruch, A., Lohning, M., and Hofer, T. (2010). Short-term memory in gene induction reveals the regulatory principle behind stochastic IL-4 expression. Mol Syst Biol *6*, 359.
Martins, G.A., Hutchins, A.S., and Reiner, S.L. (2005). Transcriptional activators of helper T cell fate are required for establishment but not maintenance of signature cytokine expression. J Immunol *175*, 5981-5985.
Miller-Jensen, K., Dey, S.S., Schaffer, D.V., and Arkin, A.P. (2011). Varying virulence: epigenetic control of expression noise and disease processes. Trends in biotechnology *29*, 517-525.
Mullen, A.C., High, F.A., Hutchins, A.S., Lee, H.W., Villarino, A.V., Livingston, D.M., Kung, A.L., Cereb, N., Yao, T.P., Yang, S.Y., and Reiner, S.L. (2001). Role of T-bet in commitment of TH1 cells before IL-12-dependent selection. Science *292*, 1907-1910.
Niesner, U., Albrecht, I., Janke, M., Doebis, C., Loddenkemper, C., Lexberg, M.H., Eulenburg, K., Kreher, S., Koeck, J., Baumgrass, R*., et al.* (2008). Autoregulation of Th1-mediated inflammation by twist1. J Exp Med *205*, 1889-1901.
O'Garra, A., Gabrysova, L., and Spits, H. (2011). Quantitative events determine the differentiation and function of helper T cells. Nat Immunol *12*, 288-294.
Openshaw, P., Murphy, E.E., Hosken, N.A., Maino, V., Davis, K., Murphy, K., and O'Garra, A. (1995). Heterogeneity of intracellular cytokine synthesis at the single-cell level in polarized T helper 1 and T helper 2 populations. J Exp Med *182*, 1357-1367.
Peine, M., Rausch, S., Helmstetter, C., Frohlich, A., Hegazy, A.N., Kuhl, A.A., Grevelding, C.G., Hofer, T., Hartmann, S., and Lohning, M. (2013). Stable T-bet(+)GATA-3(+) Th1/Th2 hybrid cells arise in vivo, can develop directly from naive precursors, and limit immunopathologic inflammation. PLoS Biol *11*, e1001633.
Pham, D., Vincentz, J.W., Firulli, A.B., and Kaplan, M.H. (2012). Twist1 regulates Ifng expression in Th1 cells by interfering with Runx3 function. J Immunol *189*, 832-840.
Raj, A., Peskin, C.S., Tranchina, D., Vargas, D.Y., and Tyagi, S. (2006). Stochastic mRNA synthesis in mammalian cells. PLoS Biol *4*, e309.
Rand, U., Rinas, M., Schwerk, J., Nohren, G., Linnes, M., Kroger, A., Flossdorf, M., Kaly-Kullai, K., Hauser, H., Hofer, T., and Koster, M. (2012). Multi-layered stochasticity and paracrine signal propagation shape the type-I interferon response. Mol Syst Biol *8*, 584.
Robinson, D., Shibuya, K., Mui, A., Zonin, F., Murphy, E., Sana, T., Hartley, S.B., Menon, S., Kastelein, R., Bazan, F., and O'Garra, A. (1997). IGIF does not drive Th1 development but synergizes with IL-12 for interferon-gamma production and activates IRAK and NFkappaB. Immunity *7*, 571-581.

Shnyreva, M., Weaver, W.M., Blanchette, M., Taylor, S.L., Tompa, M., Fitzpatrick, D.R., and Wilson, C.B. (2004). Evolutionarily conserved sequence elements that positively regulate IFN-gamma expression in T cells. Proc Natl Acad Sci U S A *101*, 12622-12627.
Sigal, A., Milo, R., Cohen, A., Geva-Zatorsky, N., Klein, Y., Liron, Y., Rosenfeld, N., Danon, T., Perzov, N., and Alon, U. (2006). Variability and memory of protein levels in human cells. Nature *444*, 643-646.
Slifka, M.K., Rodriguez, F., and Whitton, J.L. (1999). Rapid on/off cycling of cytokine production by virus-specific CD8+ T cells. Nature *401*, 76-79.
Suter, D.M., Molina, N., Gatfield, D., Schneider, K., Schibler, U., and Naef, F. (2011). Mammalian genes are transcribed with widely different bursting kinetics. Science *332*, 472-474.
Szabo, S.J., Dighe, A.S., Gubler, U., and Murphy, K.M. (1997). Regulation of the interleukin (IL)-12R beta 2 subunit expression in developing T helper 1 (Th1) and Th2 cells. J Exp Med *185*, 817-824.
Szabo, S.J., Kim, S.T., Costa, G.L., Zhang, X., Fathman, C.G., and Glimcher, L.H. (2000). A novel transcription factor, T-bet, directs Th1 lineage commitment. Cell *100*, 655-669.
Usui, T., Nishikomori, R., Kitani, A., and Strober, W. (2003). GATA-3 suppresses Th1 development by downregulation of Stat4 and not through effects on IL-12Rbeta2 chain or T-bet. Immunity *18*, 415-428.
Wei, G., Wei, L., Zhu, J., Zang, C., Hu-Li, J., Yao, Z., Cui, K., Kanno, Y., Roh, T.Y., Watford, W.T.*, et al.* (2009). Global mapping of H3K4me3 and H3K27me3 reveals specificity and plasticity in lineage fate determination of differentiating CD4+ T cells. Immunity *30*, 155-167.
Zhao, M., Zhang, J., Phatnani, H., Scheu, S., and Maniatis, T. (2012). Stochastic expression of the interferon-beta gene. PLoS Biol *10*, e1001249.
Zhu, J., Jankovic, D., Oler, A.J., Wei, G., Sharma, S., Hu, G., Guo, L., Yagi, R., Yamane, H., Punkosdy, G.*, et al.* (2012). The transcription factor T-bet is induced by multiple pathways and prevents an endogenous Th2 cell program during Th1 cell responses. Immunity *37*, 660-673.
Zhu, J., Min, B., Hu-Li, J., Watson, C.J., Grinberg, A., Wang, Q., Killeen, N., Urban, J.F., Jr., Guo, L., and Paul, W.E. (2004). Conditional deletion of Gata3 shows its essential function in T(H)1-T(H)2 responses. Nat Immunol *5*, 1157-1165.
Zhu, J., Yamane, H., and Paul, W.E. (2010). Differentiation of effector CD4 T cell populations (*). Annu Rev Immunol *28*, 445-489.

Author contributions

C.H. and M.P. designed the study, performed most experiments, analyzed data, and wrote the manuscript. M.F. and T.H. conceptualized, performed, and described mathematical modeling. A.K., A.N.H., M.A.D., Q.Z., Y.V. performed experiments. J.Z., A.R., S.H.K., and W.E.P. provided tools and advice. T.H. and M.L. designed and directed the study and wrote the manuscript.

Acknowledgements

We thank V. Holecska, S. Ebel, I. Panse, and U. Zedler for expert technical assistance and the FCCF at DRFZ for cell sorting.

This work was supported by the German Federal Ministry of Education and Research (FORSYS and e:Bio/T-Sys), the German Research Foundation (SFB618, TPC3; SFB650, TP28; LO1542/3-1 and HO02050/4-1), and the Volkswagen Foundation (Lichtenberg program to M.L.). C.H., M.P., and M.A.D. were fellows of the International Max Planck Research School for Infectious Diseases and Immunology. A.K. was supported by the National Health and Medical Research Council of Australia through a CJ Martin Biomedical Early Career Fellowship (APP1052764). A.N.H. is supported by an EMBO long-term fellowship (ALTF 116-2012) and a Marie Curie fellowship (FP7-PEOPLE-2012-IEF, Proposal 330621). J.Z. and W.E.P. are supported by the Division of Intramural Research, NIAID, NIH, USA. T.H. and M.F. are supported in part by the US National Science Foundation (NSF PHY11-25915).

The authors declare that no competing interests exist.

Figure legends

Figure 1. Individual Th cells maintain their specific rate of cytokine production

(A) Alternative models of cytokine production by T cell populations. (B) Experimental setup. (C) Th1 cells were restimulated with PMA and ionomycin. Live IFN-γ^+ cells were labeled by secretion assay and cultured with or without stimulus. Intracellular IFN-γ counterstainings were performed at the indicated time points. Percentages of IFN-γ^+ cells are indicated. (D) Scheme of the ʻrapid-switching model' that allows cells to cycle between producing and nonproducing states at rates λ and ω before production is irreversibly ceased at a rate κ. (E) Scheme of the ʻstable-production model' used to extract the IFN-γ production length distribution τ in the population. Cells become IFN-γ^+ at a rate λ. (F) Fit of the ʻstable-production model' (solid line) to the time series data of IFN-γ production (intracellular staining, dots). The brefeldin A control (cross) is modeled by leaving out the second step in the model (dashed line). (G) Model fit (simultaneously with the data from F) to the kinetics of the secreted–IFN-γ^+ cells from C (IFN-γ measured by intracellular staining). (H) The resulting production period is 5.9±3.6 h (mean production period and variability within the population). Data are representative of three independent experiments. See also Figs. S1 and S2.

Figure 2. Mathematical modeling predicts inherently distinct cytokine expression capacities of individual cells

(A) Intracellular IFN-γ detection with two different antibodies. The red line represents the one standard deviation error ellipse of the IFN-γ^+ cells corresponding to a relative measurement error of 17%. (B) Scheme of the ʻpromoter state transition model':

Cytokine transcription becomes active with rate k_{on} after stimulation and is terminally inactivated with rate k_{off}; intermittently, the promoter can switch between transcriptional on- and off-states (transcriptional bursting, $k_{\pm}$). Transcription, translation, degradation of IFN-γ mRNA and protein, and protein secretion are described with rate constants v_0, k, d_R, d_P, and d_S. (C) Decline of the mean protein amount in IFN-γ^+ cells with persistent stimulus (dots) and after removal of the stimulus (crosses) (cf. Fig. 1C) together with fits of the model in B (solid lines). (D) Correlation coefficients (crosses) calculated for the secreted–IFN-γ^+ cells and fit of the model (solid line). (E) Coefficients of variation of the distributions of IFN-γ^+ cells (crosses) and simulation of the model substantially deviating from the data (solid line). The experimental data in C–E were used simultaneously for fitting the model parameters. (F) Intracellular IFN-γ staining of Th1 cells 3 h after restimulation (blue) and simulation of the ʻpromoter state transition model' (red). (G) Scheme of the ʻdistributed production capacity model': As in B but allowing only for a single switch-on and switch-off event: The promoter switches to an on-state at a rate k_{on} and switches back to a nonproductive state after a Gamma-distributed production period τ. The IFN-γ expression capacity, defined as the product of transcription and translation rates, v_0 k, is assumed to be lognormally distributed within the cell population. (H) Lognormal distribution of the IFN-γ production capacity (v_0 k) resulting from the fit in I. (I) Fit of the model (dashed line) to the time evolution of the distribution of intracellular IFN-γ amounts within the total Th1 cell population (solid line). Data are representative of three independent experiments. See also Fig. S3.

Figure 3. Individual Th1 cells exhibit a stable quantitative memory for IFN-γ and T-bet expression

(A) Experimental setup of B–D. WT recipients of 2×10^5 LCMV-TCR^{tg} CD4$^+$Thy1.1$^+$ T cells were infected with LCMV. Thy1.1$^+$ cells were reisolated on d 10 and analyzed for T-bet expression (histogram inset; black, staining; gray, isotype control). (B) Cells were restimulated with LCMV-GP$_{64\text{-}80}$, sorted by secreted IFN-γ amounts, and cultured. (C) Frequency of IFN-γ$^+$ cells and normalized IFN-γ amount per cell in the sorted fractions on d 4 after sort. (D) Normalized T-bet amounts per cell on d 4 after sort. Representative results (B) and means + SD (C, D) of two experiments are shown. (E, F) *In vitro*-differentiated Th1 cells were sorted by secreted IFN-γ amounts and cultured with IL-2. (E) Frequency of IFN-γ$^+$ cells in the sorted fractions. (F) Normalized IFN-γ amount per cell in the sorted fractions. Representative results of three (E) and means + SD of two (F) independent experiments are shown. (G, H) *In vitro*-differentiated Th1 cells were sorted by secreted IFN-γ amounts, transferred into WT mice (1.5×10^6 cells/mouse), and reisolated on d 35. Means + SD of two independent experiments are shown. (G) Frequency of IFN-γ$^+$ cells and normalized IFN-γ amount per cell in the sorted fractions. (H) Normalized T-bet amounts per cell in the sorted fractions. (I) Experimental setup of J. WT recipients of 2×10^5 LCMV-TCR^{tg} CD4$^+$Thy1.1$^+$ T cells were infected with LCMV. Thy1.1$^+$ cells were reisolated on d 10, restimulated with LCMV-GP$_{64\text{-}80}$, sorted by secreted IFN-γ amounts, and transferred into naive WT mice (5×10^4 cells/mouse). After 16 d, secondary recipients were infected with LCMV. On d 10 after challenge infection, Thy1.1$^+$ cells were reisolated. (J) Frequency of IFN-γ$^+$ cells and normalized

IFN-γ amount per cell in the sorted fractions are shown (means + SD of n=3–4 mice). See also Figs. S4 and S5.

Figure 4. The quantitative memory for IFN-γ production is regulated at the level of transcription at individual alleles

(A–C) Th1 cells were sorted by secreted IFN-γ amounts and tracked. (A) IFN-γ mRNA upon restimulation was normalized to HPRT (means + SD). (B) On d 3 after sort, cells were restimulated. 3 h after onset, transcription was inhibited in some cells (dotted line, open symbols). IFN-γ mRNA normalized to HPRT over the course of stimulation is shown. (C) Data as in (B) with a focus on early time points after stimulation onset. Data are pooled from (A) or are representative of (B, C) two independent experiments. (D) *Ifng*$^{+/+}$ or *Ifng*$^{+/-}$ Th1 cells were sorted by secreted IFN-γ amounts and cultured. Upper panel, frequency of IFN-γ^{+} cells in sorted fractions normalized to that in unsorted cells. Lower panel, normalized IFN-γ amount per cell in the sorted fractions. Means ± SD of two independent experiments are shown. (E) Degree of DNA methylation + SD is depicted in Th1 cells sorted by graded IFN-γ secretion and analyzed by bisulfite sequencing at a CpG island corresponding to CNS -6 at the *Ifng* locus (left) and at a CpG island approximately 1 kb upstream of the *Tbx21* promoter (right). See also Fig. S4.

Figure 5. T-bet and IFN-γ expression are quantitatively correlated

(A) Th1 cells were stained intracellularly for IFN-γ, either combined with T-bet staining (left plot, colored dots) or isotype control staining (left plot, gray dots). IFN-γ expression in subpopulations with different T-bet expression is shown. Frequencies of IFN-γ^{+} cells

and geometric mean of IFN-γ in IFN-γ^+ cells (bold numbers) are indicated. Data are representative of three independent experiments. (B) TBGR Th1 cells were sorted by ZsGreen expression and cultured. (C) Frequency of IFN-γ^+ cells in the sorted fractions and IFN-γ amount per cell in the sorted fractions, both normalized to those in unsorted cells are shown as means + SD on d 4 after sort. (D) Kinetic analysis of the frequency of IFN-γ^+ cells in the sorted fractions (means ± SD). Data are pooled from three (C) or two (D) independent experiments. (E–G) TBGR LCMV-TCR^{tg} Thy1.1$^+$ Th1 cells were sorted by ZsGreen expression into T-bet^{hi} or T-bet^{lo} fractions and transferred into WT mice (2×10^6cells/mouse). (E) T-bet expression and frequency of IFN-γ^+ cells directly before transfer, both normalized to those in unsorted cells. (F) T-bet expression and frequencies of IFN-γ^+ cells, both normalized to those in unsorted controls, are shown in cells reisolated from spleens on d 29 after transfer (n = 3 mice/group). Data in E and F represent means + SD from four independent experiments. (G) Correlation of IFN-γ^+ frequency with ZsGreen expression directly after sort (purple dots) and on d 29 after transfer (blue dots). Each blue dot represents transferred cells recovered from one recipient. Data are representative of two independent experiments. The purple line shows the best fit to the data obtained directly after sort using a two-parameter model (c.f. Supplemental Experimental Procedures). The shaded region indicates the 95% confidence prediction bands. The predicted functional relationship captures the measured data on d 29. See also Fig. S6.

Figure 6. T-bet quantitatively controls IFN-γ expression in fully differentiated Th1 cells

(A) Experimental setup. Th1 cells were sorted by secreted IFN-γ amounts and transduced with a T-bet–encoding or control retrovirus. IFN-γ expression was analyzed in transduced ($hCD4^+$) cells 2 d later. (B) Frequencies of IFN-γ^+ cells and geometric mean of IFN-γ in IFN-γ^+ cells (bold numbers). (C) Relative increase in IFN-γ expression probability and per-cell amount upon T-bet overexpression. (D, E) Unsorted Th1 cells were transduced with a T-bet–encoding retrovirus and analyzed 2 d later. (D) Counterstaining of T-bet and hCD4. (E) Frequencies of IFN-γ^+ cells and geometric mean of IFN-γ in IFN-γ^+ cells (bold numbers) in cells overexpressing different amounts of hCD4, i.e. T-bet. Representative results of (B, D, E) or pooled data from (C) two independent experiments are shown.

Figure 7. Graded IFN-γ production by Th1 cells regulates bacteria killing by macrophages

(A) Th1 cells were sorted by secreted IFN-γ amounts. WT or *Ifngr1*$^{-/-}$ BM-derived macrophages were infected with *S.* Typhimurium. IFN-γ–sorted fractions were co-cultured for 36 h with infected macrophages at a 1:5 ratio, or recombinant IFN-γ (10 ng/ml) was added as a control. (B) Bacterial colonies were counted after plating macrophage lysates for 24 h. (C) Nitrite accumulation in the culture medium. (D) Sorted fractions from A were cultured without macrophages for 36 h. IFN-γ concentrations in the supernatants of 4×10^5 cells/ml are shown (dotted line, detection limit). Data are pooled from (B, D) or are representative of (C) three independent experiments.

Figure1

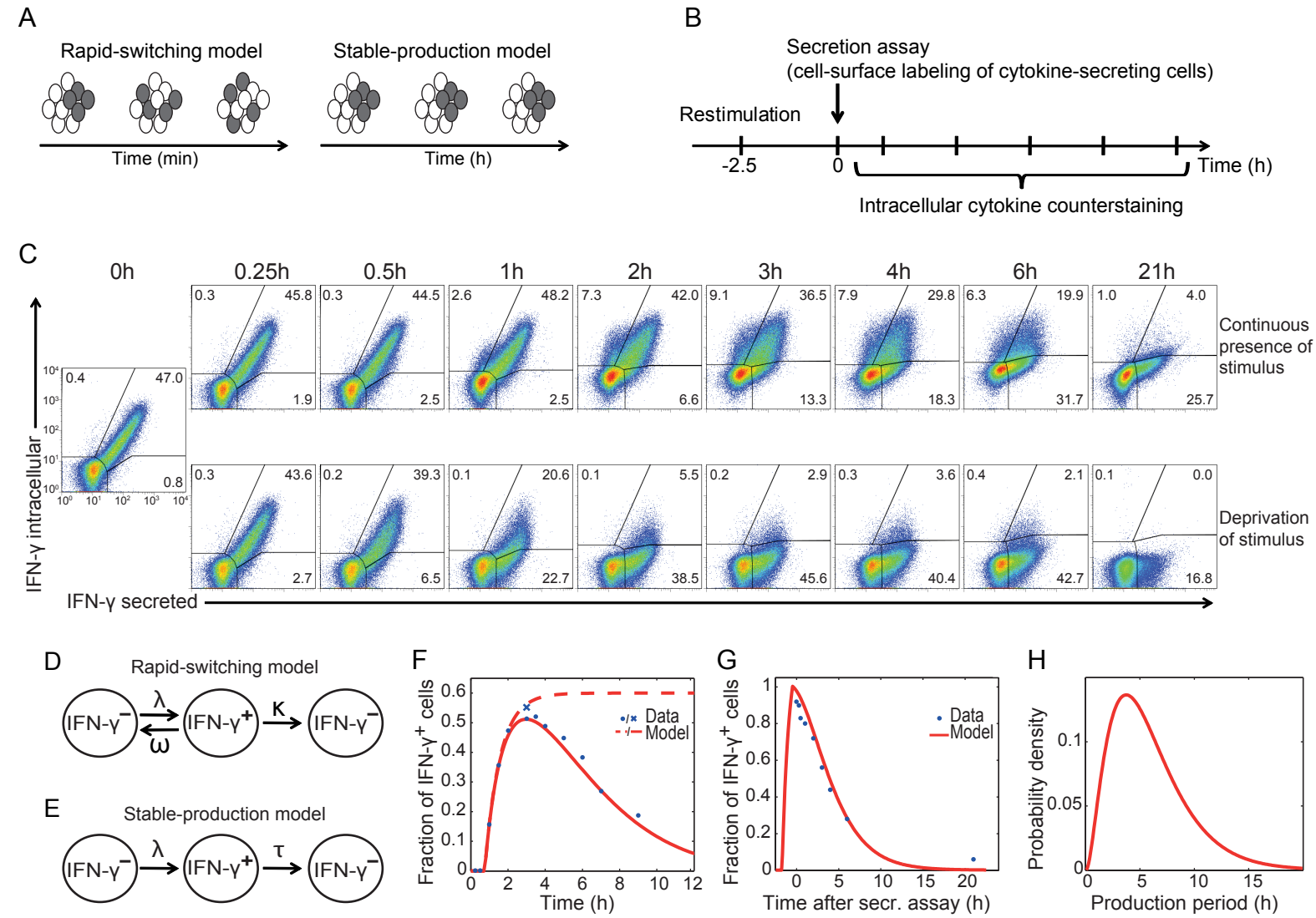
A
Rapid-switching model
Time (min)
Stable-production model
Time (h)
B
Secretion assay
(cell-surface labeling of cytokine-secreting cells)
Restimulation
-2.5
0
Time (h)
Intracellular cytokine counterstaining
C
0h
0.25h
0.5h
1h
2h
3h
4h
6h
21h
Continuous presence of stimulus
Deprivation of stimulus
IFN-γ intracellular
IFN-γ secreted

D
Rapid-switching model
IFN-γ−
λ
ω
IFN-γ+
κ
IFN-γ−

E
Stable-production model
IFN-γ−
λ
IFN-γ+
τ
IFN-γ−

F
Fraction of IFN-γ+ cells
Data
Model
Time (h)

G
Fraction of IFN-γ+ cells
Data
Model
Time after secr. assay (h)

H
Probability density
Production period (h)

Figure2

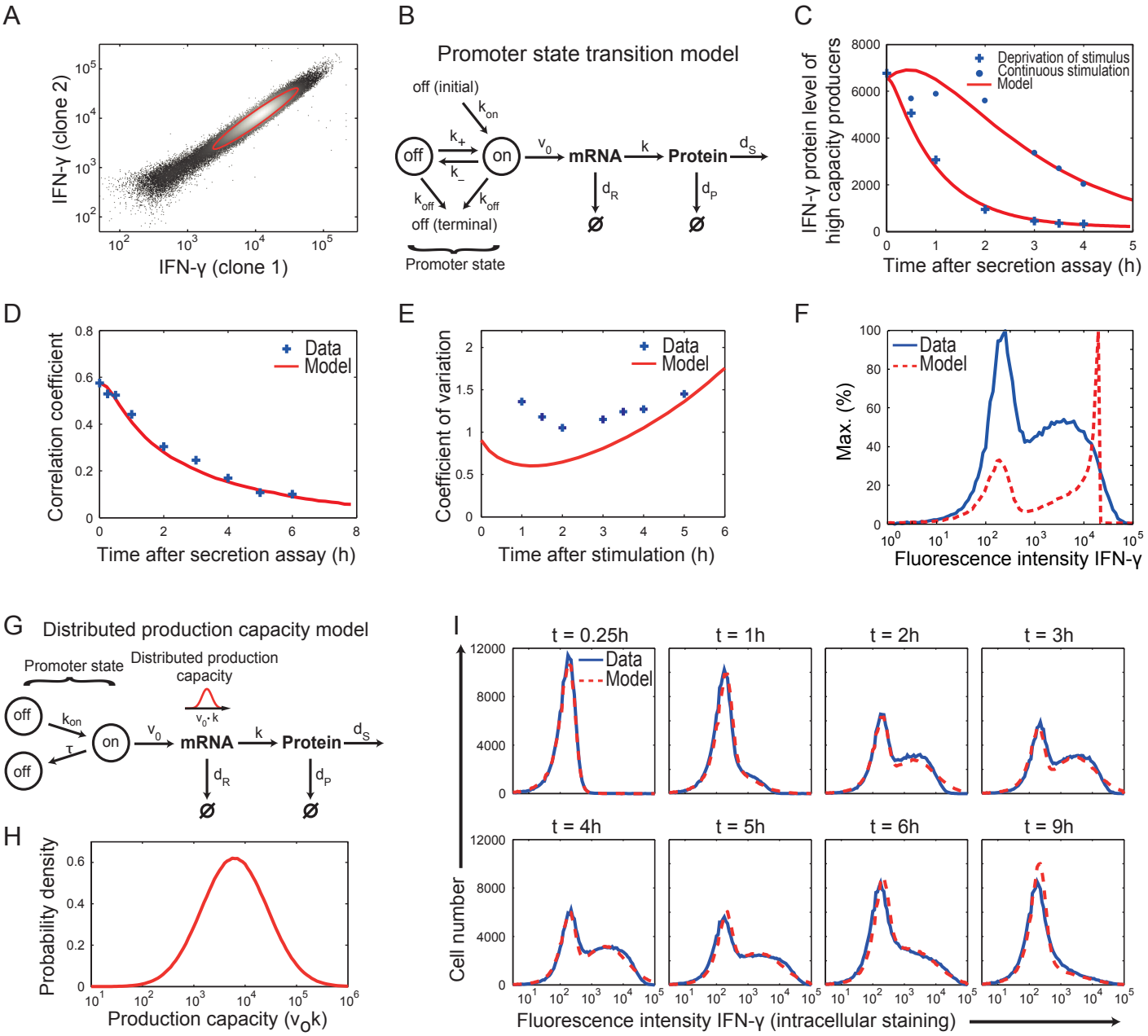
A
IFN-γ (clone 2)
IFN-γ (clone 1)
B
Promoter state transition model
off (initial)
off
on
off (terminal)
Promoter state
mRNA
Protein
C
IFN-γ protein level of high capacity producers
Deprivation of stimulus
Continuous stimulation
Model
Time after secretion assay (h)
D
Correlation coefficient
Data
Model
Time after secretion assay (h)
E
Coefficient of variation
Data
Model
Time after stimulation (h)
F
Max. (%)
Data
Model
Fluorescence intensity IFN-γ
G
Distributed production capacity model
Promoter state
Distributed production capacity
off
on
off
mRNA
Protein
H
Probability density
Production capacity (v0k)
I
t = 0.25h
t = 1h
t = 2h
t = 3h
t = 4h
t = 5h
t = 6h
t = 9h
Data
Model
Cell number
Fluorescence intensity IFN-γ (intracellular staining)

Figure3

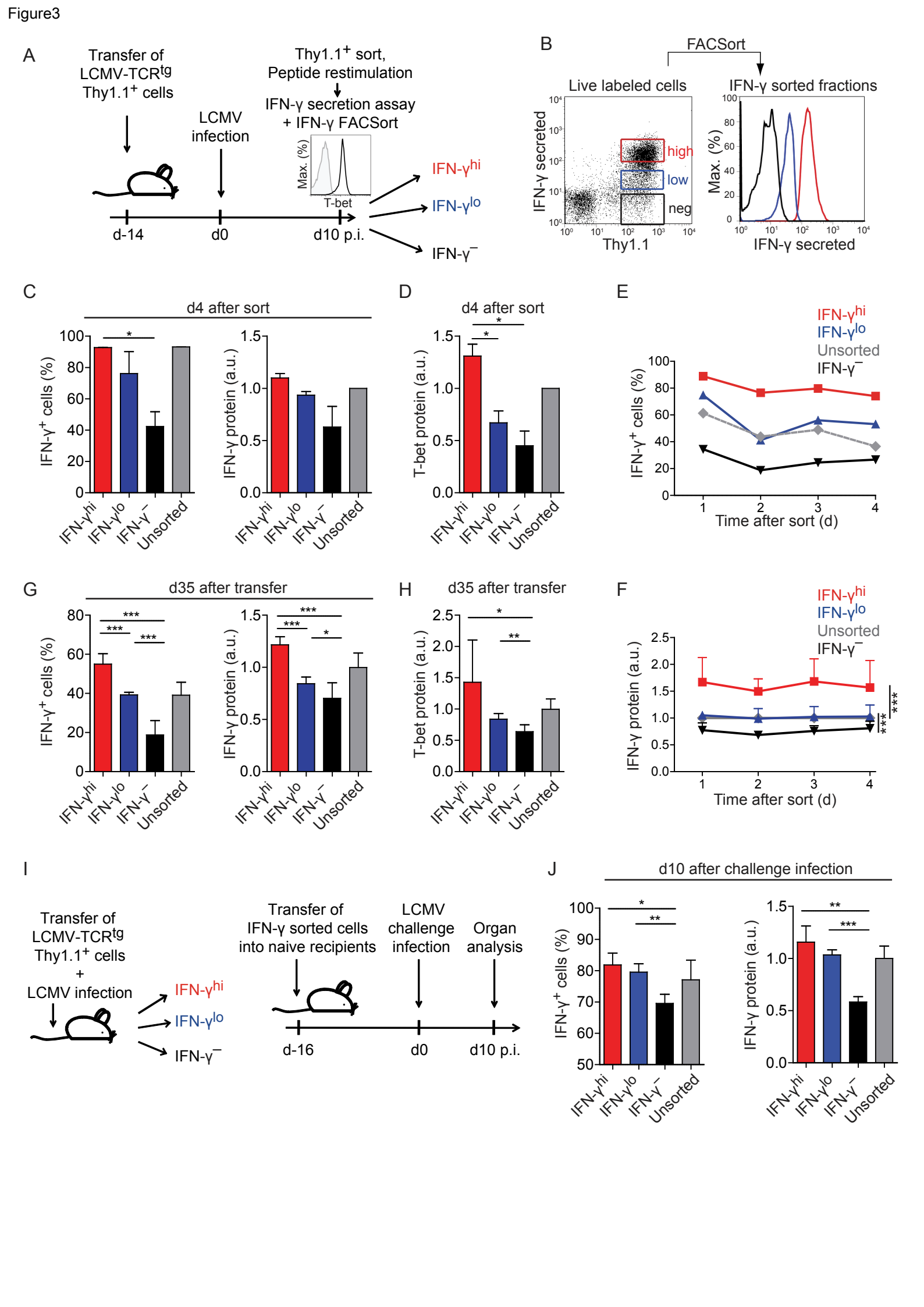
A
Transfer of LCMV-TCRtg Thy1.1+ cells
LCMV infection
Thy1.1+ sort, Peptide restimulation
IFN-γ secretion assay + IFN-γ FACSort
Max. (%)
T-bet
IFN-γhi
IFN-γlo
IFN-γ−
d-14
d0
d10 p.i.
B
FACSort
Live labeled cells
IFN-γ sorted fractions
IFN-γ secreted
high
low
neg
Thy1.1
Max. (%)
IFN-γ secreted
C
d4 after sort
IFN-γ+ cells (%)
IFN-γ protein (a.u.)
D
d4 after sort
T-bet protein (a.u.)
E
IFN-γhi
IFN-γlo
Unsorted
IFN-γ−
IFN-γ+ cells (%)
Time after sort (d)
G
d35 after transfer
IFN-γ+ cells (%)
IFN-γ protein (a.u.)
H
d35 after transfer
T-bet protein (a.u.)
F
IFN-γhi
IFN-γlo
Unsorted
IFN-γ−
IFN-γ protein (a.u.)
Time after sort (d)
I
Transfer of LCMV-TCRtg Thy1.1+ cells + LCMV infection
IFN-γhi
IFN-γlo
IFN-γ−
Transfer of IFN-γ sorted cells into naive recipients
LCMV challenge infection
Organ analysis
d-16
d0
d10 p.i.
J
d10 after challenge infection
IFN-γ+ cells (%)
IFN-γ protein (a.u.)
IFN-γhi
IFN-γlo
IFN-γ−
Unsorted

Figure4

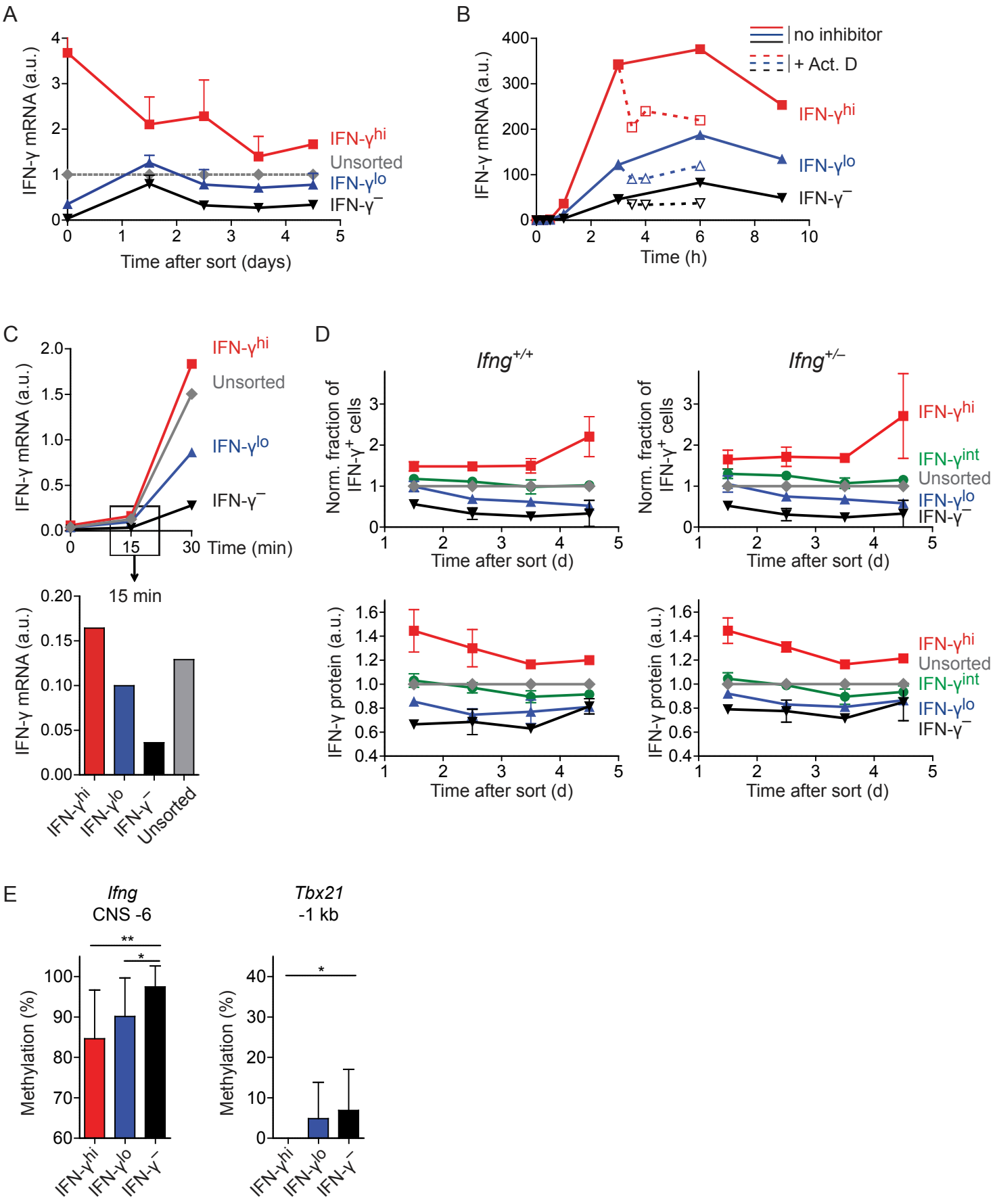
A
IFN-γ mRNA (a.u.)
Time after sort (days)
IFN-γhi
Unsorted
IFN-γlo
IFN-γ−
B
IFN-γ mRNA (a.u.)
Time (h)
no inhibitor
+ Act. D
IFN-γhi
IFN-γlo
IFN-γ−
C
IFN-γ mRNA (a.u.)
Time (min)
15 min
IFN-γhi
Unsorted
IFN-γlo
IFN-γ−
D
Ifng+/+
Ifng+/−
Norm. fraction of IFN-γ+ cells
Time after sort (d)
IFN-γ protein (a.u.)
IFN-γhi
IFN-γint
Unsorted
IFN-γlo
IFN-γ−
E
Ifng
CNS -6
Tbx21
-1 kb
Methylation (%)
IFN-γhi
IFN-γlo
IFN-γ−

Figure5

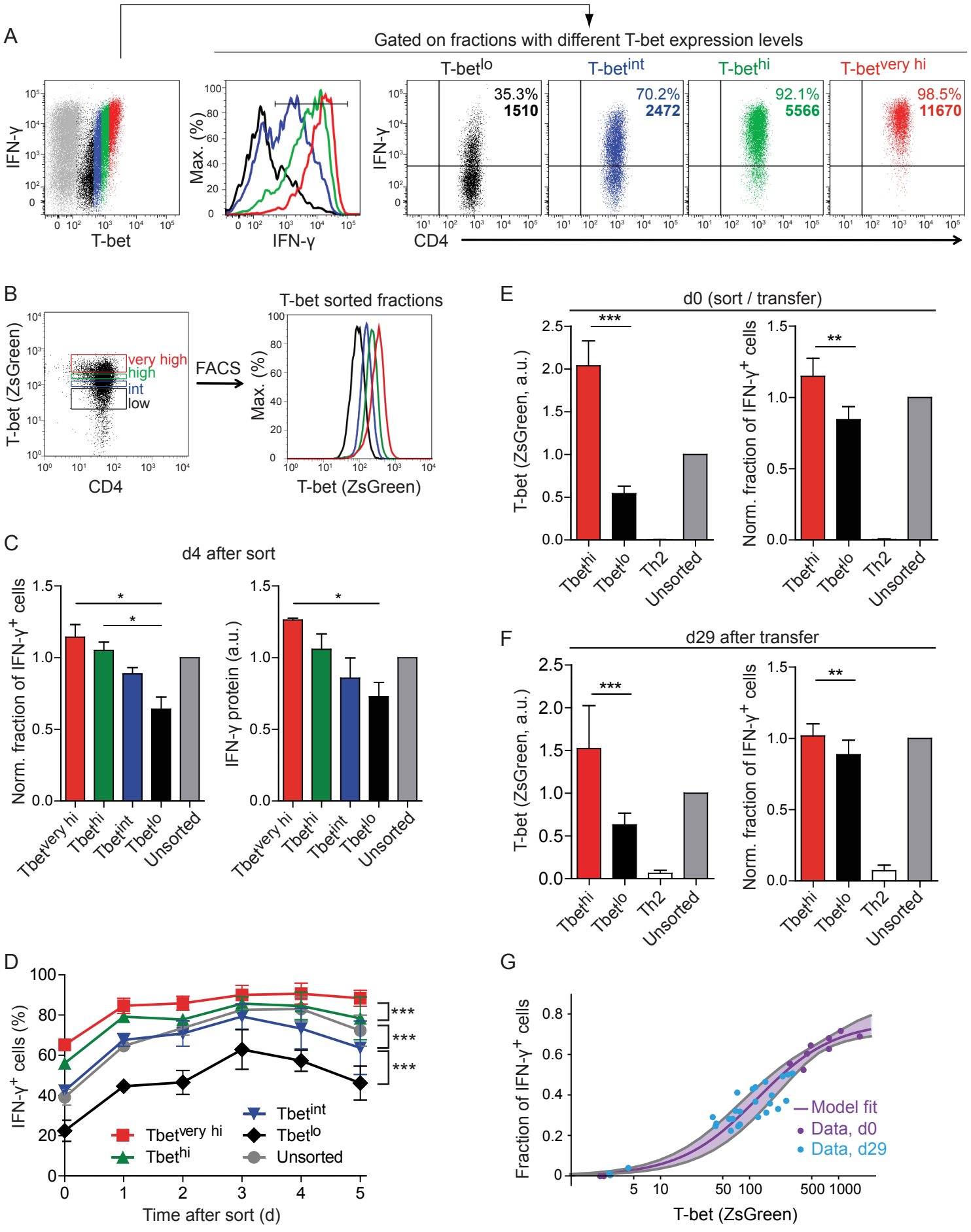
A
Gated on fractions with different T-bet expression levels
T-bet^lo
T-bet^int
T-bet^hi
T-bet^very hi
35.3%
1510
70.2%
2472
92.1%
5566
98.5%
11670
IFN-γ
T-bet
Max. (%)
CD4
B
T-bet sorted fractions
very high
high
int
low
FACS
T-bet (ZsGreen)
C
d4 after sort
Norm. fraction of IFN-γ+ cells
IFN-γ protein (a.u.)
Tbet^very hi
Tbet^hi
Tbet^int
Tbet^lo
Unsorted
D
IFN-γ+ cells (%)
Time after sort (d)
E
d0 (sort / transfer)
T-bet (ZsGreen, a.u.)
Th2
F
d29 after transfer
G
Fraction of IFN-γ+ cells
Model fit
Data, d0
Data, d29

Figure6

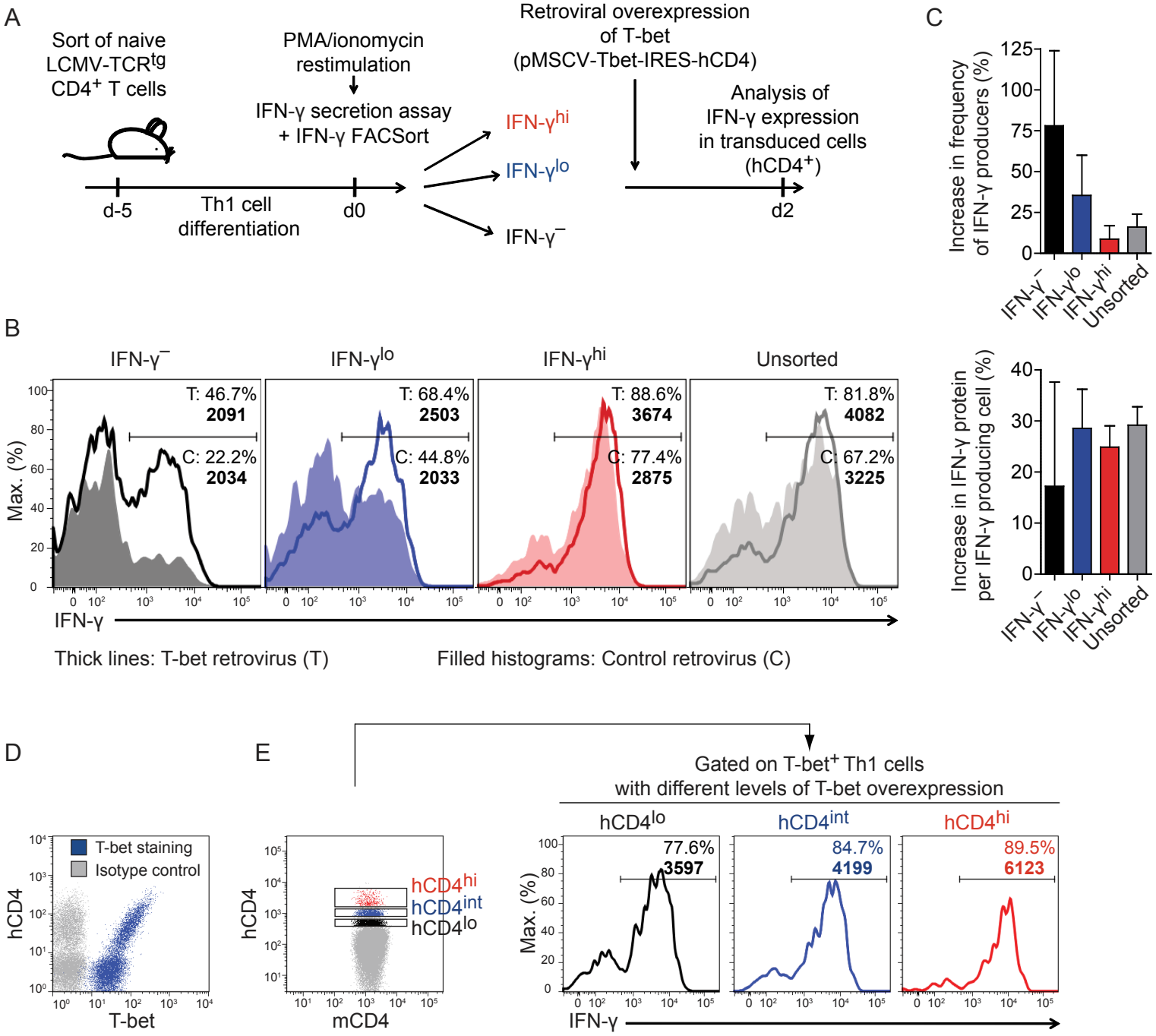
A
Sort of naive LCMV-TCRtg CD4+ T cells
PMA/ionomycin restimulation
IFN-γ secretion assay + IFN-γ FACSort
Retroviral overexpression of T-bet (pMSCV-Tbet-IRES-hCD4)
Analysis of IFN-γ expression in transduced cells (hCD4+)
IFN-γhi
IFN-γlo
IFN-γ−
d-5
Th1 cell differentiation
d0
d2
C
Increase in frequency of IFN-γ producers (%)
IFN-γ−
IFN-γlo
IFN-γhi
Unsorted
B
IFN-γ−
IFN-γlo
IFN-γhi
Unsorted
T: 46.7%
2091
C: 22.2%
2034
T: 68.4%
2503
C: 44.8%
2033
T: 88.6%
3674
C: 77.4%
2875
T: 81.8%
4082
C: 67.2%
3225
Max. (%)
IFN-γ
Thick lines: T-bet retrovirus (T)
Filled histograms: Control retrovirus (C)
Increase in IFN-γ protein per IFN-γ producing cell (%)
D
T-bet staining
Isotype control
hCD4
T-bet
E
Gated on T-bet+ Th1 cells with different levels of T-bet overexpression
hCD4lo
hCD4int
hCD4hi
77.6%
3597
84.7%
4199
89.5%
6123
Max. (%)
IFN-γ
hCD4
mCD4

Figure7

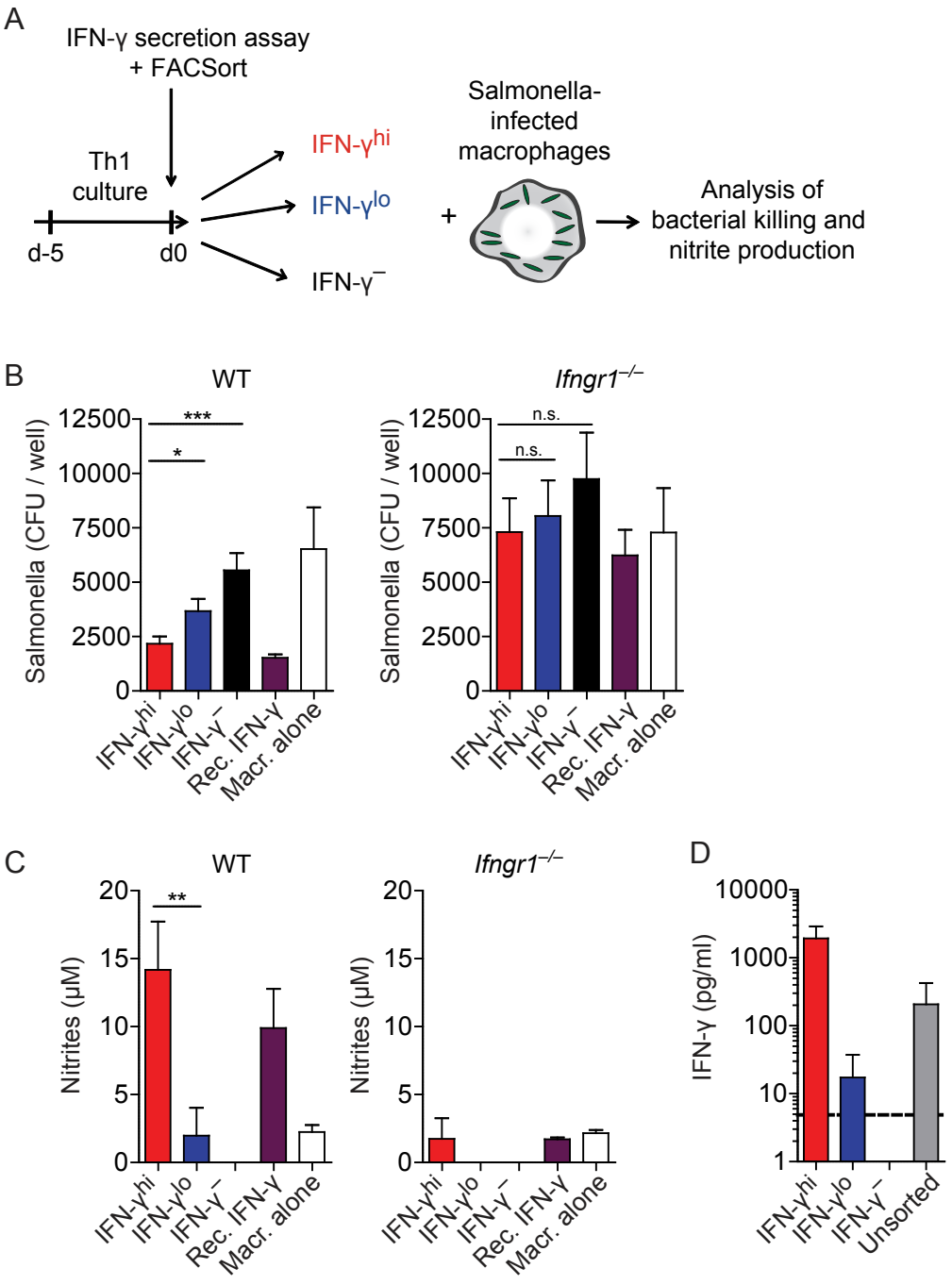
A
IFN-γ secretion assay
+ FACSort
Th1
culture
d-5
d0
IFN-γhi
IFN-γlo
IFN-γ–
Salmonella-
infected
macrophages
+
Analysis of
bacterial killing and
nitrite production
B
WT
Ifngr1–/–
Salmonella (CFU / well)
12500
10000
7500
5000
2500
0
***
*
n.s.
n.s.
IFN-γhi
IFN-γlo
IFN-γ –
Rec. IFN-γ
Macr. alone
C
WT
Ifngr1–/–
Nitrites (μM)
20
15
10
5
0
**
D
IFN-γ (pg/ml)
10000
1000
100
10
1
Unsorted

Supplemental Text & Figures

Click here to download Supplemental Text & Figures: HelmstetterSupplementalInformation.pdf

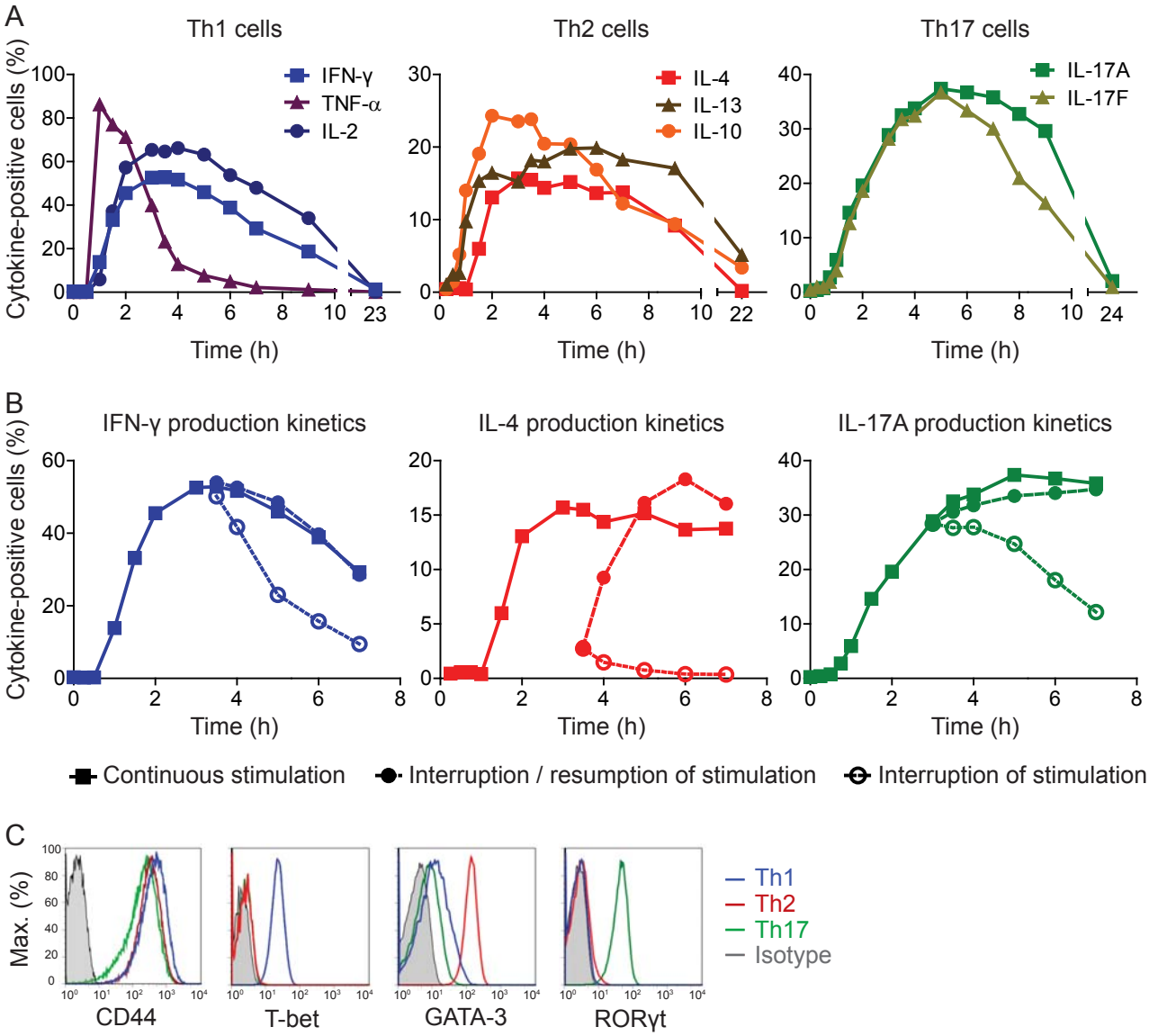

Figure S1, related to Figure 1. Differentiated Th cells segregate into stable cytokine-producing and -nonproducing subsets during one stimulation.

Naive Th cells were differentiated into Th1, Th2, or Th17 cells for 5 d. (A) Cells were restimulated with PMA and ionomycin. Cells were fixed and stained intracellularly for the indicated cytokines in a kinetic fashion. (B) A fraction of cells was deprived of the stimulus by intensive washing in ice-cold buffer at 3 h after stimulation onset. The frequency of cytokine producers was then followed in a continuous culture either without stimulus or with immediate readdition of the stimulus in comparison to the stimulation without interruption. (C) The expression of CD44, T-bet, GATA-3, and RORγt was measured by flow cytometry. Data are representative of three independent experiments.

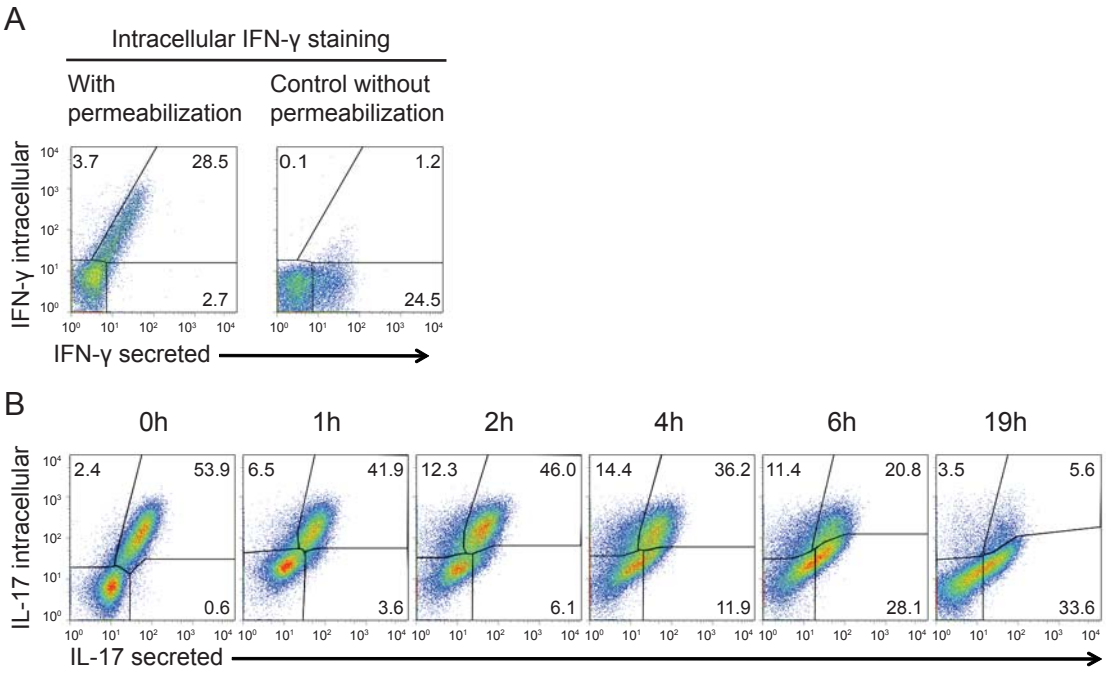
A
Intracellular IFN-γ staining
With permeabilization
Control without permeabilization
IFN-γ intracellular
3.7
28.5
2.7
0.1
1.2
24.5
IFN-γ secreted
B
0h
1h
2h
4h
6h
19h
IL-17 intracellular
2.4
53.9
0.6
6.5
41.9
3.6
12.3
46.0
6.1
14.4
36.2
11.9
11.4
20.8
28.1
3.5
5.6
33.6
IL-17 secreted

Figure S2, related to Figure 1. Secreted and intracellular cytokine detection is quantitatively correlated, and Th17 cell populations comprise stable IL-17 producers and nonproducers.

(A) IFN-γ secretion assay was performed with restimulated Th1 cells. Intracellular IFN-γ counterstaining was done either with (left) or without (right) cell permeabilization with saponin. (B) Upon restimulation of Th17 cells, live IL-17$^+$ cells were labeled by cytokine secretion assay and continuously cultured in the presence of the stimulus. Intracellular counterstainings for IL-17 were performed at the indicated time points. Data are representative of two independent experiments.

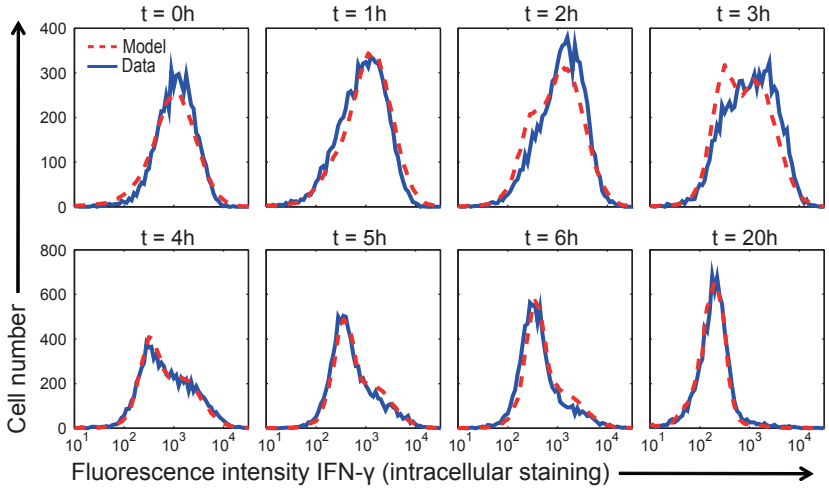
t = 0h
t = 1h
t = 2h
t = 3h
t = 4h
t = 5h
t = 6h
t = 20h
Model
Data
Cell number
Fluorescence intensity IFN-γ (intracellular staining)

Figure S3, related to Figure 2. The 'distributed production capacity' model describes the IFN-γ production dynamics of the secreted–IFN-γ^+ cells.

Fit of the 'distributed production capacity' model (dashed line; cf. Fig. 2G) to the intracellular IFN-γ expression from the secretion assay data, gated on cells with a high amount of secreted IFN-γ at $t = 0$ (solid line) using the same parameter values (except for the initial width of the IFN-γ production capacity) as for the IFN-γ production dynamics shown in Fig. 2I.

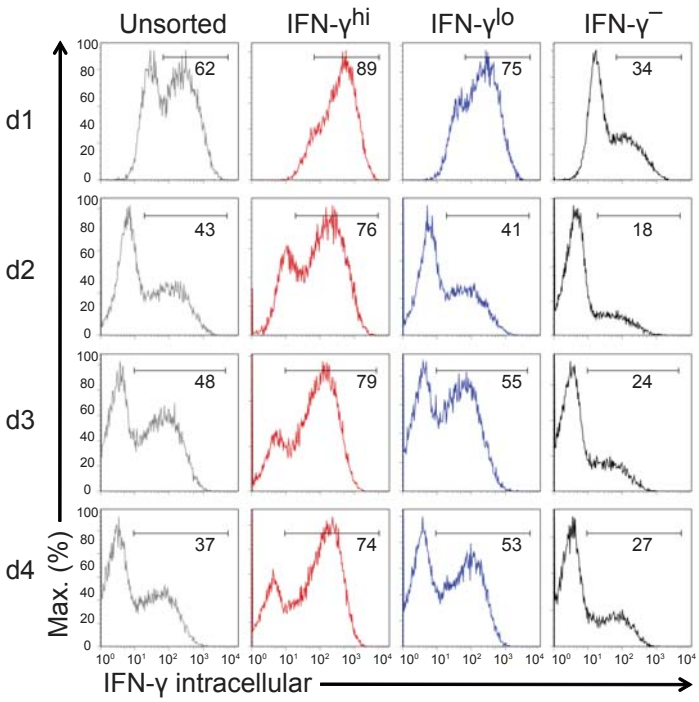
Unsorted
IFN-γhi
IFN-γlo
IFN-γ–
d1
d2
d3
d4
62
89
75
34
43
76
41
18
48
79
55
24
37
74
53
27
Max. (%)
IFN-γ intracellular

Figure S4, related to Figures 3 and 4. Th1 cells exhibit a quantitative memory for IFN-γ expression.

Th1 cells were sorted for differential IFN-γ secretion into IFN-γ^{hi}, IFN-γ^{lo}, and IFN-γ^{-} populations and cultured in the presence of IL-2. IFN-γ expression in the sorted fractions was measured upon daily restimulation. Numbers indicate the percentage of IFN-γ^{+} cells. Representative results of three independent experiments are shown.

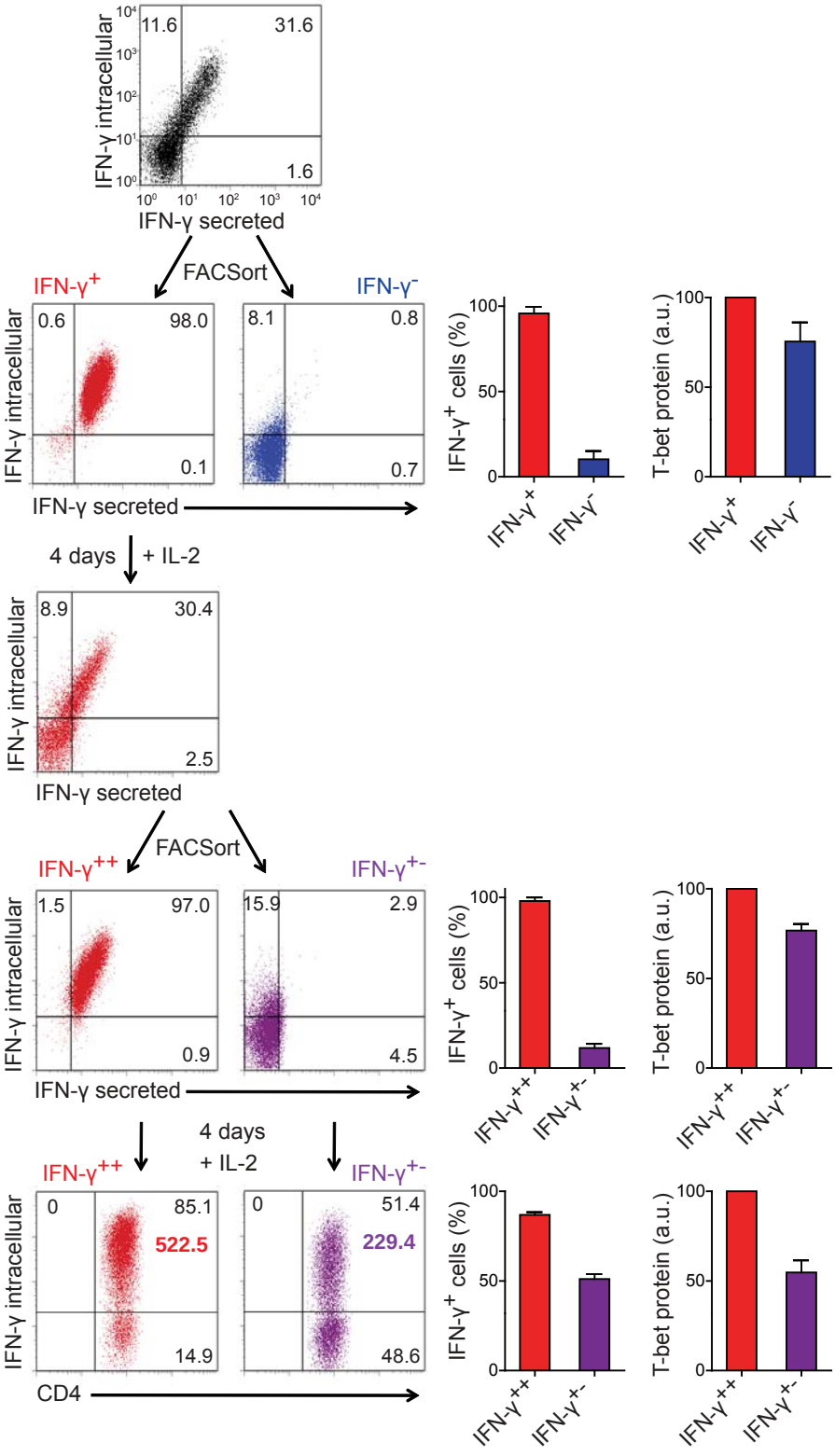
IFN-γ intracellular
IFN-γ secreted
11.6
31.6
1.6
FACSort
IFN-γ+
IFN-γ-
0.6
98.0
0.1
8.1
0.8
0.7
4 days
+ IL-2
8.9
30.4
2.5
IFN-γ++
IFN-γ+-
1.5
97.0
0.9
15.9
2.9
4.5
0
85.1
522.5
14.9
51.4
229.4
48.6
CD4
IFN-γ+ cells (%)
T-bet protein (a.u.)
100
50
0

Figure S5, related to Figure 3. IFN-γ$^+$ *bona fide* Th1 cells maintain differential capacities to express T-bet and IFN-γ.

In vitro-generated Th1 cells were restimulated and sorted into IFN-γ$^+$ and IFN-γ$^-$ fractions. IFN-γ$^+$ cells were cultured without further stimulation (medium + IL-2) for 4 d. A second restimulation followed by another IFN-γ sort was performed. IFN-γ producers and nonproducers were cultured as before, and their capacity to reexpress IFN-γ was compared on d 4. T-bet expression was analyzed directly after each sort and 4 d later and is depicted as geometric mean index relative to that of the respective IFN-γ$^+$ population. Numbers in bold and color in the dot plots show the geometric mean of IFN-γ within the IFN-γ$^+$ population. Representative results and means + SD of two independent experiments are shown.

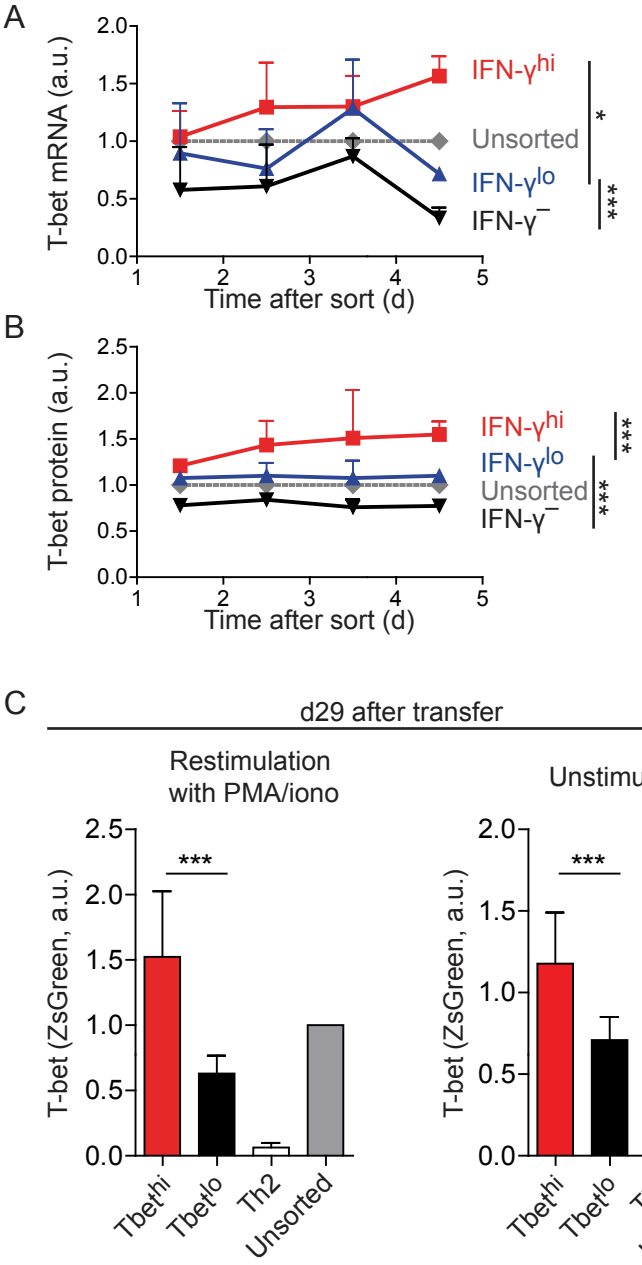
A
T-bet mRNA (a.u.)
2.0
1.5
1.0
0.5
0.0
1
2
3
4
5
Time after sort (d)
IFN-γhi
Unsorted
IFN-γlo
IFN-γ−
*
***
B
T-bet protein (a.u.)
2.5
2.0
1.5
1.0
0.5
0.0
1
2
3
4
5
Time after sort (d)
IFN-γhi
IFN-γlo
Unsorted
IFN-γ−
***
***
C
d29 after transfer
Restimulation with PMA/iono
Unstimulated
T-bet (ZsGreen, a.u.)
***
***
Tbethi
Tbetlo
Th2
Unsorted

Figure S6, related to Figure 5. Graded T-bet mRNA and protein levels are maintained in individual Th1 cells.

(A-B) Th1 cells were sorted for differential IFN-γ secretion into IFN-γ^{hi}, IFN-γ^{lo}, and IFN-γ^{-} populations and cultured in the presence of IL-2. (A) T-bet mRNA normalized to HPRT relative to that in unsorted cells is shown over time. (B) Geometric mean index of T-bet protein is shown over time. Pooled data from two independent experiments are shown. (C) TBGR LCMV-TCR^{tg} $Thy1.1^{+}$ Th1 cells were sorted for ZsGreen (i.e. T-bet) expression into $T\text{-}bet^{hi}$ or $T\text{-}bet^{lo}$ fractions and transferred into WT mice. Transferred cells isolated from spleens on d 29 after transfer were analyzed for T-bet expression by flow cytometry either with (left) or without (right) restimulation. Data represent means + SD pooled from four independent experiments.

Supplemental Table S1, related to Figures 1 and 2. Parameter estimates and confidence bounds.

Rapid-switching model

Parameter	Best-fit	95 % confidence bounds
$\bar{\tau}$	0.71 h	(0.50, 0.85) h
λ	0.87 h^{-1}	(0.71, 1.45) h^{-1}
ω	0 h^{-1}	(0, 0.09) h^{-1}
κ	0.16 h^{-1}	(0.15, 0.19) h^{-1}

Stable-production model

Parameter	Best-fit	95 % confidence bounds
$\bar{\tau}$	0.70 h	(0.50, 0.78) h
λ	1.0 h^{-1}	(0.73, 1.14) h^{-1}
τ: mean	5.9 h	(5.2, 6.0) h
τ: $\sqrt{\text{variance}}$	3.6 h	(3.4, 4.8) h

Promoter state transition model

Parameter	Best-fit[1] (used data: Fig. 2 C, D, E)	Best-fit (used data: Fig. 2 C, D)	95 % confidence bounds[2] (used data: Fig. 2 C, D)
k_{on} [3]	0.9 h^{-1}	0.9 h^{-1}	
k_+ [4]	2.0 h^{-1}	8.0 h^{-1}	(0, ∞) h^{-1}
k_-	0.69 h^{-1}	0.0092 h^{-1}	(0, 1.39) h^{-1}
d_R [5]	0.83 h^{-1}	0.80 h^{-1}	(0.42, 1.08) h^{-1}
$d_P + d_S$ [4, 5]	4.3 h^{-1}	4.23 h^{-1}	(1.3, ∞) h^{-1}
k_{off}	0.65 h^{-1}	0.70 h^{-1}	(0.45, 1.57) h^{-1}

Distributed production capacity model

Parameter	Best-fit
initial delay $\bar{\tau}$	0.58 h
μ [6]	8.75
σ [6]	1.47
mean [7]	4.2 h
$\sqrt{\text{variance}}$ [7]	2.5 h
ratio of producing cells	0.59
k_{on}	1.60 h^{-1}
d_R [8]	1.1 h^{-1}
$d_P + d_S$ [8]	5.9 h^{-1}

[1] Confidence bounds not calculated because this model is not describing the data
[2] The corresponding bootstrap sample was also used to calculate the model prediction that less than 7 % of the CV generated by the model was due to transcriptional bursting (c.f. supplemental text)
[3] Fixed in accordance with the corresponding rates in the rapid-switching and stable-production models
[4] Importantly, these non-identifiabilities have no effect on the two important conclusions inferred from the promoter state transition model: Firstly, the model fails to account both for the CV of the distribution of IFN-γ expression levels (Fig. 2E) and for the shape of this distribution (Fig. 2F). Secondly, using bootstrap we obtain a confidence bound for the contribution of transcriptional bursting to the CV, showing that it is smaller than 7 % and can therefore be neglected in the distributed production capacity model (see Supplemental Experimental Procedures for more details).
[5] Without loss of generality, it was assumed in the model fits that dP + dS > dR (fast cytokine secretion rate dS); the data just constrain at least one of the two decay rates (protein or RNA decay rate) to be sufficiently slow while the other one can be fast
[6] Parameters of the log-normal distribution for the production capacity (v_0 k)
[7] Mean and $\sqrt{\text{variance}}$ of the gamma distribution for the production time τ
[8] Fixed in accordance with the corresponding rates in the promoter state transition model

Supplemental Experimental Procedures

Mice

DO11.10 ovalbumin-TCR-transgenic (tg) mice (Murphy et al., 1990) on the BALB/c background or LCMV-TCR^{tg} (SMARTA1) (Oxenius et al., 1998) Thy1.1^{+} mice on the C57BL/6 background, which express a TCR specific for the LCMV epitope GP_{61-80}, or *Ifngr1*$^{-/-}$ mice (Muller et al., 1994) were used as organ donors for the isolation of splenocytes, lymph node cells, and bone marrow cells. TBGR mice on the C57BL/6 background (Zhu et al., 2012) were crossed to SMARTA1 Thy1.1^{+} mice and were used as organ donors. C57BL/6 mice or TBGR Thy1.2^{+} mice were used as recipients in adoptive cell transfer experiments. Mice were bred under SPF conditions at the Charité animal facility, Berlin. All mouse experiments were performed at the Charité University Medicine, in accordance with the German law for animal protection, with permission from the local veterinary office, and in compliance with the guidelines of the Institutional Animal Care and Use Committee.

Viruses and bacteria

LCMV. The LCMV-Armstrong strain was propagated on BHK cells, and virus stocks were titrated by standard immunofocus assays on MC57G cells.

***S.* Typhimurium**. *S.* Typhimurium SL1344 was grown statically at 37 °C in Luria-Bertani (LB) broth for 16–18 h. Macrophages were infected with an MOI of 1:10 for 3 h, followed by 1 h incubation with media containing gentamycin (100 μg/ml, Gibco) to kill extracellular bacteria. Upon co-culture with IFN-γ–sorted Th1 cells for 36 h, supernatants were collected and macrophages were lysed with 1% Triton X-100 (Sigma). To determine the number of replicating bacteria, macrophage lysate was serially diluted in PBS and plated onto LB agar plates supplemented with 25 μg/ml streptomycin. Plates were incubated at 37 °C for 24 h, and colonies

were counted. Macrophage nitrite production was analyzed in the culture supernatant using Griess reagent (Sigma). The absorbance at 550 nm was compared to a $NaNO_2$ standard curve.

Primary T cell cultures

Naive $CD4^+CD62L^{hi}CD44^{lo}$ T cells were sorted from pooled spleen and lymph node cells by magnetic-activated cell sorting or FACS and cultured in RPMI 1640+GlutaMax-I supplemented with 10% (v/v) FCS (Gibco), penicillin (100 U/ml; Gibco), streptomycin (100 µg/ml; Gibco), and ß-mercaptoethanol (50 ng/ml; Sigma) in the presence of APCs and 0.5 µg/ml $Ova_{323-339}$ peptide or LCMV-GP_{64-80}, respectively (R. Volkmer, Institute for Med. Immunology, Charité). For Th1 cell differentiation, 3 ng/ml IL-12 and 10 µg/ml anti–IL-4 (11B11) were added. For Th2 cell differentiation, 30 ng/ml IL-4, 10 µg/ml anti–IL-12 (C17.8), and 10 µg/ml anti–IFN-γ (AN18.17.24) were added. For Th17 cell differentiation, 20 ng/ml IL-6, 1 ng/ml TGF-β, 10 ng/ml IL-23, 10 µg/ml anti–IL-4, and 10 µg/ml anti–IFN-γ were used. All recombinant cytokines were purchased from R&D Systems. Cell cultures were split on d 3 and analyzed on d 5.

Bone-marrow derived macrophages

Bone marrow was isolated from hind legs of C57BL/6 mice or *Ifngr1*$^{-/-}$ mice by flushing bones with DMEM. Bone marrow cells were cultured at a concentration of 1×10^6cells/ml in DMEM supplemented with 10% (v/v) FCS (Sigma), 5% (v/v) horse serum (Invitrogen), L-glutamine (2mM, GE Healthcare), HEPES (10mM, Gibco), sodium pyruvate (1mM, Biochrome), and 20% (v/v) M-CSF-containing L929 cell culture supernatants. On d 6, macrophages were harvested, plated at a concentration of 2×10^5 cells/ml, and infected 24 h later.

Intracellular cytokine staining and flow cytometry

On d 5 of culture or at the indicated analysis time points, cells were purified by underlaying Histopaque (Sigma-Aldrich) and performing high density centrifugation (400g at 20°C for 20 min). Cells were then restimulated with PMA (5 ng/ml) and ionomycin (500 ng/ml) for 2.5 – 3 h with addition of brefeldin A (5 µg/ml; all from Sigma-Aldrich) at 30 min, followed by fixation in 2% formaldehyde (Merck). For *ex vivo* sorting of IFN-γ–producing cells (Fig. 3), an antigen-specific restimulation using the GP_{64-80} peptide was performed for 4 h. In some experiments, the transcription inhibitor actinomycin D (Sigma-Aldrich) was added at a concentration of 5 µg/ml to cells restimulated with PMA and ionomycin.

Intracellular staining was performed in PBS/0.2% BSA containing 0.05% saponin (Sigma-Aldrich) for permeabilization. Samples were stained with antibodies against CD4 (RM4-5), Thy1.1 (OX-7), CD44 (IM7), IFN-γ (XMG1.2, AN18.17.24), IL-2 (JES6-5H4), TNF-α (MPG-XT22), IL-4 (11B11), IL-10 (JES5-16E3), IL-13 (38213.11), IL-17A (TC11-18H10), IL-17F (eBio-18F10).

Samples were sorted on a FACSAria II and acquired on a FACSCanto II (Becton Dickinson). Data were analyzed with Flow Jo (Tree Star).

Transcription factor staining

T-bet, GATA-3, and RORγt protein amounts were analyzed using FoxP3 staining buffer set (eBioscience) according to the manufacturer's instructions. Briefly, cells were stained with PerCP-conjugated anti-CD4 and then fixed with 1x Fixation/Permeabilization buffer, followed by intracellular staining with PE-conjugated anti–T-bet (4B10), Alexa-647–conjugated anti–GATA-3 (TWAJ, both from eBioscience) or PE-conjugated anti-RORγt (Q31-378 from BD) in 1x permeabilization buffer. Cells were washed in 1x permeabilization buffer and analyzed.

Cytokine secretion assay

The cytometric cytokine secretion assay was performed as described before (Assenmacher et al., 1998; Lohning et al., 2003). Briefly, cells were restimulated for 2.5 h to 4 h, followed by labeling with an IFN-γ– or IL-17–specific capture matrix (Miltenyi Biotec). The capture matrix-labeled cells were kept in 37°C warm medium for 20 min. Matrix-captured cytokine was stained on the cell surface with anti–IFN-γ-PE or anti–IL-17-biotin followed by anti–biotin-PE (Miltenyi Biotec).

Upon FACS sort, cells were continuously cultured in medium containing recombinant mouse IL-2 (5ng/ml, R&D Systems) and recombinant mouse IL-7 (5ng/ml, Peprotech), if not indicated otherwise.

RNA isolation and real-time PCR

Total RNA was isolated from the sorted cell populations using the NucleoSpin RNA II kit (Macherey-Nagel), according to the manufacturer's instructions. Reverse transcription into cDNA was performed using the Taqman kit (Roche Diagnostics). For real-time PCR, the FastStart DNA Master SYBR Green I kit (Roche Diagnostics) was used. For normalization, the mRNA expression values of the gene of interest were divided by the mRNA expression values of a housekeeping gene, i.e. hypoxanthine guanine phosphoribosyl transferase (HPRT). Data were evaluated using Lightcycler software (LightCycler3 Data Analysis).

Primer sequences:

HPRT, GCTGGTGAAAAGGACCTCT and CACAGGACTAGAACACCTGC;

Ifng, CAACAACATAAGCGTCATT and ATTCAAATAGTGCTGGCAGA;

Tbet, TCCTGCAGTCTCTCCACAAGT and CAGCTGAGTGATCTCTGCGT.

Mathematical modeling

Rapid-switching model (Fig. 1D): A certain fraction p_0 of the cells stays quiescent for the whole duration of the stimulation. The remaining cells stay quiescent only for the time period $\bar{\tau}$ and can then cycle between an IFN-γ producing (state B) and nonproducing state (state A) at rates λ and ω. IFN-γ positive cells can switch off production irreversibly at a rate *k*. The master equation for this system reads

$$\dot{p}(A,t) = -\lambda\, p(A,t) + \omega\, p(B,t)$$

$$\dot{p}(B,t) = \lambda\, p(A,t) - (\omega + k)\, p(B,t),$$

with $p(A,\bar{\tau}) = 1 - p_0$ and $p(B,\bar{\tau}) = 0$. For the secretion assay positive cells the initial conditions are changed to $p_{\mathrm{sec}}(B,t_{\mathrm{sec}}) = 1$ and $p_{\mathrm{sec}}(A,t_{\mathrm{sec}}) = 0$, where t_{sec} denotes the time point of the secretion assay.

To fit both probabilities $p(B,t)$ and $p_{\mathrm{sec}}(B,t)$ to the experimental data, we obtained first the time series of secretion-assay positive cells by gating for the cells that produced IFN-γ at t = 0 and determined the fraction of remaining producers using the intracellular staining. We then estimated all model parameters by fitting both probabilities simultaneously to the kinetics of the secretion-assay positive cells and the time series of IFN-γ positive cells in the whole population using the trust-region-reflective algorithm of MathWorks MATLAB's optimization toolbox (the data is shown in Figs. 1F and 1G). To additionally constrain the model, we included in the fit the experimental control where the secretion inhibitor brefeldin A was added to the culture (data point depicted as a cross in Fig. 1F). In the model this corresponds to the solution of the above master equation for the case $\omega = k = 0$. We used a parametric bootstrap approach to resample

the data (n = 10,000; resampling of the residuals) and subsequently refitted the model resulting in an (95 % confidence level) upper bound on ω of 0.09/h. The best-fit values and confidence bounds for all parameters can be found in Supplemental Table S1.

Stable-production model (Fig. 1E): As in the rapid-switching model, a fraction p_0 of the cells stays quiescent for the whole duration of the stimulation. Following stimulation, the remaining cells stay quiescent for the time period $\bar{\tau}$ and then become IFN-γ producers at a rate λ. After the production period τ (assumed as a gamma-distributed random variable), IFN-γ production ceases. The model admits the following analytical solution for the probability to produce IFN-γ at time t

$$P(t) = \int_0^\infty p(t,\tau)\Gamma(\tau,k,\theta)d\tau\,,$$

where $\Gamma(\tau,k,\theta)$ is the gamma distribution with rate parameter k and scale parameter θ and $p(t,\tau)$ is the production probability with constant τ, given by

$$p(t,\tau) = (1-p_0)\cdot\begin{cases} 0, & t \le \bar{\tau} \\ 1-e^{-\lambda(t-\bar{\tau})}, & t > \bar{\tau} \wedge t < \tau + \bar{\tau} \\ \left(1-e^{-\lambda\,\tau}\right)e^{-\lambda(t-\tau-\bar{\tau})}, & t \ge \tau + \bar{\tau}. \end{cases}$$

For constant τ, the probability to find a cell producing IFN-γ at the time point of the secretion assay t_{sec} and at time t is

$$p^+(t,\tau) = (1-p_0)\cdot\begin{cases} 0, & t \le \bar{\tau} \\ 1-e^{-\lambda(t-\bar{\tau})}, & t > \bar{\tau} \wedge t \le t_{\text{sec}} \\ 1-e^{-\lambda(t_{\text{sec}}-\bar{\tau})}, & t > t_{\text{sec}} \wedge t \le \tau + \bar{\tau} \\ e^{-\lambda(t-\tau-\bar{\tau})} - e^{-\lambda(t_{\text{sec}}-\bar{\tau})}, & t > \tau + \bar{\tau} \wedge t \le t_{\text{sec}} + \tau \\ 0, & t > t_{\text{sec}} + \tau, \end{cases}$$

for $t_{\text{sec}} < \bar{\tau} + \tau$ and otherwise

$$p^+(t,\tau) = (1-p_0)\cdot\begin{cases} 0, & t \le t_{\text{sec}} - \tau \\ e^{-\lambda(t_{\text{sec}}-\tau-\bar{\tau})}(1-e^{-\lambda(t-t_{\text{sec}}+\tau)}), & t > t_{\text{sec}} - \tau \wedge t \le t_{\text{sec}} \\ e^{-\lambda(t_{\text{sec}}-\bar{\tau})}(e^{\lambda(t_{\text{sec}}+\tau-t)}-1), & t > t_{\text{sec}} \wedge t \le t_{\text{sec}} + \tau \\ 0, & t > t_{\text{sec}} + \tau. \end{cases}$$

The probability $P^+(t)$ for a gamma distributed τ is then calculated analogous to $P(t)$.

Both probabilities were fitted to the experimental data as described above for the rapid-switching model (Figs. 1F and 1G). The resulting distribution for the production period τ is shown in Fig. 1H. Assessment of the parameter confidence bounds was done via bootstrapping as described above for the Rapid-switching model. The resulting confidence bounds for all parameters as well as their best-fit values can be found in Supplemental Table S1.

Promoter state transition model (Fig. 2B): To determine the parameters of the promoter state transition model, we first computed the correlation coefficients of IFN-γ protein amounts measured at two different time points (autocorrelation; cf. Fig. 2D). In order to correct for any positive correlation that is due to background effects (e.g. surface-bound IFN-γ), the intracellular IFN-γ amounts for different levels of surface IFN-γ were normalized by the corresponding IFN-γ amounts of a control population that was treated equally except that the permeabilization step prior to the intracellular staining was left out (no saponin added). In the following we will first briefly discuss the analytical tractable case of vanishing k_{on} and k_{off} rates in steady state to gain some intuition and then turn to the full model. While analytical formulas for both the autocorrelation function and the coefficient of variation can be obtained readily for the steady state distribution of the model in the case of vanishing k_{on} and k_{off} rates, we relied for the full-

time-dependent model on simulations of a large number of cells (n = 100,000) for the calculation of these quantities in the full model (see further below).

The autocorrelation function R for the promoter state transition model with $k_{on} = k_{off} = 0$ has been calculated elsewhere (Raj et al., 2006). It is given by the inverse Fourier transformation of

$$\hat{R}(\omega) = \left|\hat{h}_P(\omega)\right|^2 \left|\hat{h}_R(\omega)\right|^2 \hat{R}_R(\omega),$$

where the hat denotes the Fourier transform and

$$h_P(t) = H(t)\, k\, e^{-(d_P+d_S)t},$$

$$h_R(t) = H(t)\, v_0\, e^{-d_R t},$$

$$R_R(t) = \frac{k_{\text{on}} k_{\text{off}}}{(k_{\text{on}} + k_{\text{off}})^2} e^{-(k_{\text{on}}+k_{\text{off}})|t|},$$

with the Heaviside function H. The coefficient of variation η in this case is given by (Raj et al., 2006):

$$\eta^2 = \frac{k_{\text{off}}}{k_{\text{on}}} \frac{d_R(d_P + d_S)}{d_R + d_P + d_S} \frac{d_R + d_P + d_S + k_{\text{on}} + k_{\text{off}}}{(d_R + k_{\text{on}} + k_{\text{off}})(d_P + d_S + k_{\text{on}} + k_{\text{off}})}.$$

The decline of the mean protein amount P in IFN-γ producers after withdrawal of the PMA and ionomycin stimulus (Fig. 2C, crosses) leading to an immediate transition to the promoter off state in the model is independent on k_{on} and k_{off}; it is given by

$$P(t) = \text{const.} \cdot \left(\frac{1}{d_R} e^{-d_R\, t} \left(e^{d_R\, t_{sec}} - 1\right) - \frac{1}{d_P + d_S} e^{-(d_P+d_S)\, t} \left(e^{(d_P+d_S)\, t_{sec}} - 1\right) \right),$$

where t_{sec} denotes the time at which the secretion assay was performed.

In order to calculate the autocorrelation function, the coefficient of variation, and the switching-off kinetics under continuous PMA and ionomycin stimulation (in contrast to stimulus withdrawal, this means continuous shuttling between promoter on and off states according to the full model also after the secretion assay was conducted) for the case of non-vanishing rates k_{on} and k_{off}, we relied on the numerical simulation of the trajectories for a large number of cells (n = 100,000). To this end, switching-on and switching-off times for every simulated cell were drawn from the exponential distributions defined by the rates k_{on}, k_{off} , k_{+} and k_{-}. Within the resulting time intervals, the RNA (R) and protein (P) kinetics were computed analytically based on the solution of the following two ordinary differential equation systems.

In the case of the promoter becoming active at time point t_a at which RNA and protein amounts are given by R_0 and P_0, respectively, the system is described by

$$\dot{R}(t) = v_0 - d_R R(t),$$

$$\dot{P}(t) = k\, R(t) - d_P P(t),$$

$$R(t_a) = R_0,$$

$$P(t_a) = P_0,$$

for all time points t before the promoter becomes inactive again. Accordingly, for a transition to the inactive promoter state occurring at time point t_i, protein and RNA amounts are governed by

$$\dot{R}(t) = v_0 d_R R(t),$$

$$\dot{P}(t) = k\, R(t) - d_P P(t),$$

$$R(t_i) = R_0,$$

$$P(t_i) = P_0,$$

for all time points *t* before the promoter (possibly) becomes active again.

The simulated quantities were then fitted to the data shown in Figs. 2C, D and E using the trust-region-reflective algorithm of MathWorks MATLAB's optimization toolbox. While describing both the switching-off kinetics (Fig. 2C) and the autocorrelation function (Fig. 2D) accurately, the model fails to account for the large variability (as quantified by the coefficients of variation shown in Fig. 2E) of the IFN-γ producers (more than one thousand random initial values for the fitted parameters were tried). This necessitated the introduction of an additional source of variability into the model, which lead us to introduce cell-to-cell differences in the individual production capacities (defined as the product of transcription and translation rates, $v_0\ k$) of the cells (c.f. Distributed production capacity model). Such a model extension results in an additional 'cell-extrinsic' source of variability, but does not affect the (average) switching off kinetics or the autocorrelation function (Figs. 2C, D). It also does not alter the 'cell-intrinsic' contribution to the variability in the amount of expressed IFN-γ formed by asynchronous switching-on and switching-off times as well as transcriptional bursting (realized in the model by continuous shuttling between the non-terminal off-state and the on-state). In the next step we quantified the relative contribution of transcriptional bursting to the cell-intrinsic variability. For this purpose we refitted the promoter-state transition model solely to the data in Figs. 2C and D. We then used parametric bootstrapping as described above (n = 1,000 samples) and for each bootstrap sample calculated the ratio between the predicted coefficient of variation (at t = 3h) setting k_{-} = 0 (thereby switching off transcriptional bursting in the model) and the full model. The resulting 95 % confidence bounds for this prediction is (93, 100)%, meaning that transcriptional bursting is predicted to contribute less than 7 % to the cell-intrinsic variability while its major part is formed

by asynchronous switching-on and switching-off times (more than 93%). This allowed us to ignore transcriptional bursting in the distributed production capacity model (Fig. 2G).

Distributed production capacity model (Fig. 2G): For the modeling of the cytokine amounts we constrained the model to allow only for a single switch-on and switch-off event: The promoter switches to an on-state at a rate k_{on}, and, similar to the stable-production model, switches back to a non-productive state after the period τ (assumed as a gamma-distributed random variable). Since the above promoter state transition model failed to reproduce the broad distribution of IFN-γ levels, we introduced a lognormal distribution for the IFN-γ expression capacity, defined as the product of transcription and translation rates, v_0 k. The corresponding model distributions in the amount of IFN-γ were obtained by simulating a large number of cells (n = 300,000) and subsequent addition of the background caused by the IFN-γ negative cells. For each simulated cell, a switch-on time t_1 and a switch-off time t_2 was drawn and the protein level P at time t was calculated according to the analytical solution

$$P(t) = \frac{k\, v_0}{d_P + d_S - d_R}$$

$$\times \begin{cases} 0, & t \le t_1 \\ \left(\frac{1}{d_R}\left(1 - e^{-d_R(t-t_1)}\right) - \frac{1}{d_P + d_S}\left(1 - e^{-(d_P+d_S)(t-t_1)}\right)\right), & t > t_1, t \le t_2 \\ \left(\frac{1}{d_R} e^{-d_R(t-t_1)}\left(e^{d_R(t_2-t_1)} - 1\right) - \frac{1}{d_P + d_S} e^{-(d_P+d_S)(t-t_1)}\left(e^{(d_P+d_S)(t_2-t_1)} - 1\right)\right), & t > t_2. \end{cases}$$

We then used simulated annealing to directly fit the model to the time series of observed distributions of intracellular IFN-γ (Fig. 2I). The same approach was also used to fit the amount of intracellular IFN-γ for the secretion-assay high cells (at every time point defined as the 15 % brightest cells in the staining for secreted IFN-γ at t = 0 h).

We used the following function to describe the functional relationship of ZsGreen expression Z and the frequency of IFN-γ producers I (c.f. Fig. 5G):

$$I = I_{\max} \frac{Z}{K + Z}.$$

The two parameters $I_{\max}$ and K were estimated using the ZsGreen expression values and the corresponding frequency of IFN-γ producers directly after the sort. In order to illustrate that the implied functional relationship between both variables also holds true for the data obtained 29 days after the transfer, we calculated the 95% confidence prediction bands by bootstrapping the data and subsequent refitting.

Supplemental References

Assenmacher, M., Lohning, M., Scheffold, A., Manz, R.A., Schmitz, J., and Radbruch, A. (1998). Sequential production of IL-2, IFN-gamma and IL-10 by individual staphylococcal enterotoxin B-activated T helper lymphocytes. Eur J Immunol *28*, 1534-1543.

Lohning, M., Richter, A., Stamm, T., Hu-Li, J., Assenmacher, M., Paul, W.E., and Radbruch, A. (2003). Establishment of memory for IL-10 expression in developing T helper 2 cells requires repetitive IL-4 costimulation and does not impair proliferation. Proc Natl Acad Sci U S A *100*, 12307-12312.

Muller, U., Steinhoff, U., Reis, L.F., Hemmi, S., Pavlovic, J., Zinkernagel, R.M., and Aguet, M. (1994). Functional role of type I and type II interferons in antiviral defense. Science *264*, 1918-1921.

Murphy, K.M., Heimberger, A.B., and Loh, D.Y. (1990). Induction by antigen of intrathymic apoptosis of CD4+CD8+TCRlo thymocytes in vivo. Science *250*, 1720-1723.

Oxenius, A., Bachmann, M.F., Zinkernagel, R.M., and Hengartner, H. (1998). Virus-specific MHC-class II-restricted TCR-transgenic mice: effects on humoral and cellular immune responses after viral infection. Eur J Immunol *28*, 390-400.

Raj, A., Peskin, C.S., Tranchina, D., Vargas, D.Y., and Tyagi, S. (2006). Stochastic mRNA synthesis in mammalian cells. PLoS Biol *4*, e309.

Zhu, J., Jankovic, D., Oler, A.J., Wei, G., Sharma, S., Hu, G., Guo, L., Yagi, R., Yamane, H., Punkosdy, G.*, et al.* (2012). The transcription factor T-bet is induced by multiple pathways and prevents an endogenous Th2 cell program during Th1 cell responses. Immunity *37*, 660-673.

Inventory of Supplemental Information

Supplemental Figures and Tables

Main text Figure 1 is supported by Supplemental Figure 1.

Main text Figure 1 is supported by Supplemental Figure 2.

Main text Figure 2 is supported by Supplemental Figure 3.

Main text Figures 3 and 4 are supported by Supplemental Figure 4.

Main text Figure 3 is supported by Supplemental Figure 5.

Main text Figure 5 is supported by Supplemental Figure 6.

Main text Figures 1 and 2 are supported by Supplemental Table 1.

Supplemental Experimental Procedures

Supplemental References